HIGH-RESOLUTION AI MAPPING OF CLIMATE PROJECTIONS FOR MARINE PROTECTED AREAS IN THE MARITIMES

E. McKee, R. Danielson, B. DeTracey, E. Kenchington, M. Skinner, B. Greenan, and Z. Wang

Bedford Institute of Oceanography
1 Challenger Drive
Dartmouth, Nova Scotia
Canada B2Y 4A2

2025

Canadian Technical Report of
Hydrography and Ocean Sciences 406

Fisheries and Oceans Canada | Pêches et Océans Canada

Canada

Canadian Technical Report of Hydrography and Ocean Sciences

Technical reports contain scientific and technical information of a type that represents a contribution to existing knowledge but which is not normally found in the primary literature. The subject matter is generally related to programs and interests of the Oceans and Science sectors of Fisheries and Oceans Canada.

Technical reports may be cited as full publications. The correct citation appears above the abstract of each report. Each report is abstracted in the data base *Aquatic Sciences and Fisheries Abstracts.*

Technical reports are produced regionally but are numbered nationally. Requests for individual reports will be filled by the issuing establishment listed on the front cover and title page.

Regional and headquarters establishments of Ocean Science and Surveys ceased publication of their various report series as of December 1981. A complete listing of these publications and the last number issued under each title are published in the *Canadian Journal of Fisheries and Aquatic Sciences*, Volume 38: Index to Publications 1981. The current series began with Report Number 1 in January 1982.

Rapport technique canadien sur l'hydrographie et les sciences océaniques

Les rapports techniques contiennent des renseignements scientifiques et techniques qui constituent une contribution aux connaissances actuelles mais que l'on ne trouve pas normalement dans les revues scientifiques. Le sujet est généralement rattaché aux programmes et intérêts des secteurs des Océans et des Sciences de Pêches et Océans Canada.

Les rapports techniques peuvent être cités comme des publications à part entière. Le titre exact figure au-dessus du résumé de chaque rapport. Les rapports techniques sont résumés dans la base de données *Résumés des sciences aquatiques et halieutiques*.

Les rapports techniques sont produits à l'échelon régional, mais numérotés à l'échelon national. Les demandes de rapports seront satisfaites par l'établissement auteur dont le nom figure sur la couverture et la page de titre.

Les établissements de l'ancien secteur des Sciences et Levés océaniques dans les régions et à l'administration centrale ont cessé de publier leurs diverses séries de rapports en décembre 1981. Vous trouverez dans l'index des publications du volume 38 du *Journal canadien des sciences halieutiques et aquatiques*, la liste de ces publications ainsi que le dernier numéro paru dans chaque catégorie. La nouvelle série a commencé avec la publication du rapport numéro 1 en janvier 1982.

Canadian Technical Report of Hydrography
and Ocean Sciences 406

2025

High-resolution AI mapping of climate projections for Marine Protected Areas in the Maritimes

by

E. McKee, R. Danielson, B. DeTracey, E. Kenchington, M. Skinner,
B. Greenan, and Z. Wang

Science Branch, Maritimes Region
Bedford Institute of Oceanography
Fisheries and Oceans Canada
1 Challenger Drive
Dartmouth, Nova Scotia Canada B2Y 4A2

Cat. No. Fs97-18/406E-PDF ISBN 978-0-660-79299-6 ISSN 1488-5417

Correct Citation for this publication:

McKee, E., Danielson, R., DeTracey, B., Kenchington, E., Skinner, M., Greenan, B., and Wang, Z. 2025. High-resolution AI mapping of climate projections for Marine Protected Areas in the Maritimes. Can. Tech. Rep. Hydrogr. Ocean Sci. 406: v + 29 p.

TABLE OF CONTENTS

ABSTRACT iv
RÉSUMÉ v
1. Introduction 1
2. Methodology and datasets 4
2.1 Datasets 4
2.2 Methodology 6
3. Results and Discussion 7
3.1 The Gully MPA 7
3.2 Laurentian Channel MPA 11
3.3 St. Anns Bank MPA 14
3.4 Basin Head MPA 16
3.5 Banc-des-Américains MPA 19
3.6 Musquash Estuary MPA 22
4. Conclusions 25
5. Acknowledgements 25
6. References 26
7. Appendix 29

ABSTRACT

McKee, E., Danielson, R., DeTracey, B., Kenchington, E., Skinner, M., Greenan, B., and Wang, Z. 2025. High-resolution AI mapping of climate projections for Marine Protected Areas in the Maritimes. Can. Tech. Rep. Hydrogr. Ocean Sci. 406: v + 29 p.

Statistical downscaling and bias correction of a 22-member global climate model ensemble, generated at approximately 100 km horizontal native resolution in Phase 6 of the Coupled Model Intercomparison Project (CMIP6), enhance the resolution of ocean projections for Marine Protected Areas (MPAs), and provide critical insights for marine conservation under climate change. By investigating downscaled projections across four CMIP6 scenarios (representing a spectrum of high to low emissions reduction paths: SSP1-2.6, SSP2-4.5, SSP3-7.0 and SSP5-8.5), this study sought greater precision in the ocean temperature, salinity, mixed layer depth (MLD) and bottom current changes that could threaten ecosystem structure and marine species. A neural network mapping technique was applied to six MPAs on Canada's east coast: the Gully, Laurentian Channel, St. Anns Bank, Basin Head, Banc-des-Américains, and the Musquash Estuary. Across these MPAs, sea surface temperature (SST) is projected to rise by between 1.5°C and 5.5°C by 2080-2100, with bottom temperatures increasing by between 1.9°C and 6.2°C in some regions. These warming trends can endanger temperature-sensitive species, such as cold-water corals and northern wolffish, potentially driving shifts in species distributions. Salinity changes are less pronounced but show declines that are more notable under higher emissions scenarios, with sea surface salinity dropping by up to 1 PSU in most MPAs. MLD exhibits a consistent shallowing trend, reflecting intensified surface warming and freshening. Predicted bottom currents, however, remain largely unchanged across scenarios. Particularly the Gully, Laurentian Channel, and St. Anns Bank demonstrate notable warming and salinity changes. These findings underscore the precision available from neural networks when delivering actionable data at scales relevant to scientists and policymakers. Because this statistical downscaling and bias correction was trained using historical data, improvements in CMIP6 ocean model projections should be possible in principle, but continued monitoring and adaptive management strategies to safeguard marine ecosystems are also needed.

RÉSUMÉ

McKee, E., Danielson, R., DeTracey, B., Kenchington, E., Skinner, M., Greenan, B., and Wang, Z. 2025. High-resolution AI mapping of climate projections for Marine Protected Areas in the Maritimes. Can. Tech. Rep. Hydrogr. Ocean Sci. 406: v + 29 p.

La réduction de l'échelle statistique et la correction du biais d'un ensemble de 22 modèles climatiques mondiaux, généré à une résolution native horizontale d'environ 100 km lors de la phase 6 du Projet de comparaison de modèles couplés (CMIP6), ont amélioré la résolution des projections océaniques pour les zones de protection marines (ZPM) et ont fourni des renseignements essentiels pour la conservation marine dans le contexte des changements climatiques. En examinant les projections à échelle réduite pour quatre scénarios du CMIP6 (représentant un spectre de scénarios de réduction des émissions élevées à faibles : SSP1-2.6, SSP2-4.5, SSP3-7.0 et SSP5-8.5), cette étude visait à obtenir une plus grande précision de la température océanique, de la salinité, de la profondeur de la couche de mélange et des changements dans les courants de fond qui pourraient menacer la structure écosystémique et les espèces marines. Une technique de cartographie de réseau neuronal a été appliquée à six ZPM sur la côte est du Canada, à savoir le Gully, le chenal Laurentien, le banc de Sainte-Anne, Basin Head, le Banc-des-Américains et l'estuaire de la Musquash. Dans ces ZPM, selon les projections, la température de la surface de la mer augmenterait de 1,5 à 5,5 °C d'ici 2080-2100, avec une augmentation de la température au fond de 1,9 à 6,2 °C dans certaines régions. Ces tendances de réchauffement peuvent mettre en danger les espèces sensibles à la température, comme les coraux d'eau froide et le loup à tête large, ce qui peut entraîner des changements dans la répartition des espèces. Les changements de salinité étaient moins prononcés, mais présentaient des déclins qui étaient plus marquants dans les scénarios d'émissions plus élevées, avec une baisse de la salinité de la surface de la mer allant jusqu'à 1 USP dans la plupart des ZPM. Il y avait également une tendance constante vers une réduction de la profondeur de la couche de mélange, reflétant une intensification du réchauffement et de la dessalure de la surface. Les courants de fond prédits sont toutefois demeurés en grande partie inchangés dans tous les scénarios. En particulier, le Gully, le chenal Laurentien et le banc de Sainte-Anne ont présenté des changements notables de réchauffement et de salinité. Ces résultats soulignent la précision possible des réseaux neuronaux lorsqu'ils fournissent des données exploitables à des échelles pertinentes pour les scientifiques et les décideurs. Comme cette réduction de l'échelle statistique et cette correction du biais ont été entraînées à l'aide des données antérieures, des améliorations dans les projections du modèle océanique CMIP6 devraient être possibles en principe, mais une surveillance continue et des stratégies de gestion adaptative pour protéger les écosystèmes marins sont également nécessaires.

1. Introduction

Canada's oceans are closely connected to and impacted by the changing atmosphere and global climate. Oceans are affected by both seasonal and year-to-year climate variability, as well as long-term climate change. As Canada's oceans absorb this heat and carbon dioxide, they become warmer and more acidic (Greenan et al. 2019), summer sea ice in the Arctic decreases, and marine heatwaves become more frequent. Ocean currents and mixing redistribute the heat and carbon dioxide absorbed at the sea surface to deeper waters, causing further changes to marine ecosystems that are expected to last for decades or longer. Many marine species are expected to respond to such climate changes through shifts in depth and latitudinal distribution (Pinsky et al. 2013, Boyce et al. 2022, Czich et al. 2023, Lawlor et al. 2024, S. Wang et al. 2024), as well as by shifting the seasonal timing of events such as spawning (Brickman and Shackell 2024). As evidence of adaptation through evolutionary processes remains limited, these changes may render spatially-fixed protective measures less effective as conditions evolve in the future.

Marine Protected Areas (MPAs) and Other Effective Area-based Conservation Measures (OECMs), such as marine refuges, provide long-term biodiversity conservation benefits for species, habitats, and ecosystems. An MPA is a discrete area of the ocean that is legally protected and managed to achieve the long-term conservation of nature. MPAs may allow some current and future activities depending on their impacts on the ecological features being protected. An OECM helps to protect important species, their habitats, and ecosystems, including unique and significant aggregations of corals and sponges. Its primary purpose and management may differ from those of an MPA, but OECMs are intended to be in place long-term, ensuring a lasting contribution to marine conservation.

The Coupled Model Intercomparison Project Phase 6 (CMIP6) represents the latest generation of climate models developed by the global scientific community (Eyring et al. 2016). These models are designed to simulate Earth's climate system and its various components, including the atmosphere, oceans, land surface, and cryosphere. CMIP6 builds upon earlier climate projection exercises, and provides enhanced capabilities and improved representations of key processes. CMIP6 model results encompass a wide range of variables and scenarios, allowing researchers to explore different aspects of past, present, and future conditions. This includes simulations of historical climate conditions and projections of future climate change under various greenhouse gas emission scenarios. The previous CMIP5 exercise used Representative Concentration Pathways (RCPs) to represent greenhouse gas concentration trajectories, whereas CMIP6 introduces a greater diversity of socio-economic scenarios or Shared Socio-economic Pathways (SSPs) from SSP1-2.6 to SSP5-8.5 (IPCC 2021). Here, 2.6, 4.5, 7.0 and 8.5 are chosen to capture a range of possible future scenarios, but continue to refer to global radiative forcing in Watts per meter squared.

The CMIP6 models provide SSP-forced climate simulations that are global and free-running (i.e., without data assimilation). These simulations are an important basis for impact assessments, but they are performed at relatively large spatial scales (~100 km) and each model has systematic biases compared to observations (e.g., Z. Wang et al. 2024). Biases are often

associated with processes that a climate model does not resolve, and when finer scales are required to assess the impact on ocean species, systematic adjustments are sought using downscaling and bias correction approaches (e.g., Drenkard et al. 2021). Dynamical downscaling (DD) involves a nested regional climate model that uses CMIP6 model output as its boundary conditions, but like global climate models, this method incurs a large computational cost and does not necessarily include bias correction (Drenkard et al. 2021). Although climate models do not assimilate observations, an ocean data assimilation system like GLORYS12 (Lellouche et al. 2021) performs systematic adjustments that can be applied to climate model output as a parameterization. Thus, an alternative to DD is to train a neural network by taking GLORYS12 as a reference and training a relationship or mapping from CMIP6 predictors to corresponding GLORYS12 predictands. Aspects of downscaling and bias correction are both addressed by neural networks that offer greater precision by design (Danielson et al. 2025). Parameterizations that are obtained using historical data can then be applied to projections to 2100. With the caveat that these parameterizations are fixed in time, local climate change impacts can be assessed at higher resolution and with greater precision across CMIP6 models.

There are currently 14 *Oceans Act* MPAs across Canada, comprising over 480,000 km² or roughly 8% of Canada's marine and coastal areas. This report focuses on selected MPAs in the Canadian Maritime provinces and attempts to provide estimates for the future oceanographic conditions in these areas using a CPU-based AI mapping approach. The MPAs investigated are the Gully, Laurentian Channel, St. Anns Bank, Basin Head, Banc-des-Américains, and the Musquash Estuary (Fig. 1).

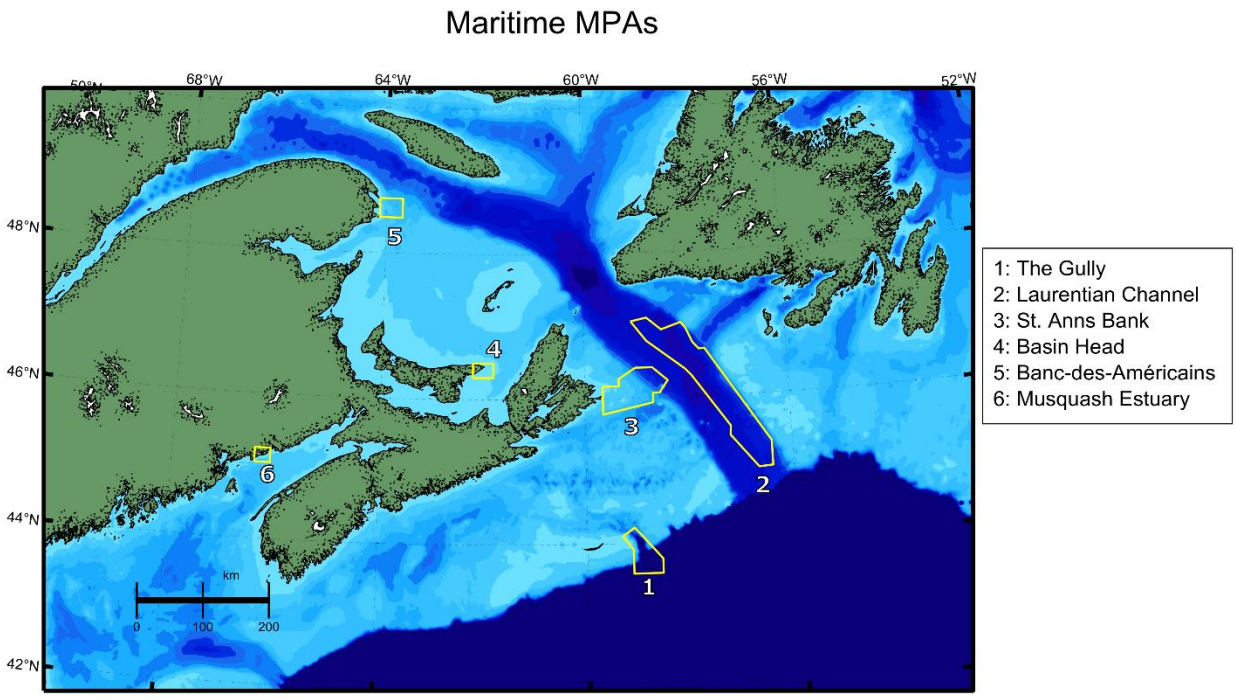

Figure 1: Locations of the six Maritime and Atlantic province MPAs examined in this study (outlined in yellow).

(1) Gully MPA
The Gully MPA is located to the east of Nova Scotia's Sable Island, covering an area of approximately 2,363 km², accounting for 0.04% of the total coverage of the Marine Conservation Targets. The Gully is the largest underwater canyon in the western North Atlantic. Its ecosystem includes shallow sandy banks, a deep-water canyon with feeder canyons incising the steep slopes, and portions of the continental slope and abyssal plain, providing habitat for a wide diversity of species (DFO 2022). The Gully's size, shape, and location affect currents and local circulation patterns, concentrating nutrients and small organisms within the canyon.

(2) Laurentian Channel MPA
The Laurentian Channel MPA is located off the southwest coast of Newfoundland and Labrador, covering an area of approximately 11,580 km², accounting for 0.20% of the total coverage of the Marine Conservation Targets. The Laurentian Channel is a deep submarine valley more than 1,200 km in length, stretching from the intersection of the St. Lawrence and Saguenay Rivers to the edge of the continental shelf off Newfoundland. This MPA includes the seabed, the subsoil to a depth of five meters, and the water column above the seabed. The Laurentian Channel MPA provides important habitat for a variety of marine species, and it has been described as having the highest sea-pen concentrations in the entire Newfoundland and Labrador Shelves bioregion (DFO 2011).

(3) St. Anns Bank MPA
The St. Anns Bank MPA is located to the east of Cape Breton Island, covering an area of approximately 4,364 km², accounting for 0.08% of the total coverage of the Marine Conservation Targets. The St. Anns Bank is an exceptional habitat with many ecologically and biologically significant features. It has the highest annual sea surface temperature range on the Scotian Shelf and provides important habitat for both commercial and non-commercial species. St. Anns Bank is part of an important migration corridor for fish and marine mammals moving in and out of the Gulf of St. Lawrence and St. Lawrence Estuary (Ford and Serdynska 2013).

(4) Basin Head MPA
The Basin Head MPA is located at the eastern tip of Prince Edward Island, covering an area of approximately 9 km², accounting for less than 0.01% of the total coverage of the Marine Conservation Targets. It contains a unique coastal environment, including a type of Irish moss that may be endemic to this MPA. This variety of Irish moss does not attach to the bottom and is significantly larger than plants found elsewhere (Joseph et al. 2021). Additionally, it has a higher concentration of carrageenan, an important thickening agent used in products such as ice cream and sunscreen.

(5) Banc-des-Américains MPA
The Banc-des-Américains MPA is located in the Gulf of St. Lawrence, near Cape Gaspé and Bonaventure Island to the west, covering an area of approximately 1,000 km², accounting for 0.02% of the total coverage of the Marine Conservation Targets. This area includes the entire submarine rocky ridge known as the American Bank, as well as the adjacent plains. The bank peaks at 12 meters below the water surface and consists of two shelves separated by a sharp ridge. The area supports a wide range of marine habitats and species, including many forage

species (Faille et al. 2023). The Gaspé current, which carries nutrients, is a primary reason for the variety of habitats and marine species found in this area.

(6) Musquash Estuary MPA

The Musquash Estuary MPA is located 20 km southwest of Saint John, New Brunswick, with its boundary defined by the water level at low tide. Its approximate area is ~7 km², accounting for less than 0.01% of the total coverage of the Marine Conservation Targets. The Musquash Estuary is unique among Bay of Fundy estuaries due to its size, expansive salt marshes, and natural condition. It is the largest ecologically intact estuary in the Bay of Fundy (DFO 2025).

2. Methodology and datasets

An Earth System Model (ESM) provides numerical simulations of coupled global biogeochemical and physical systems. This involves a sustained effort to develop each component and tune the model as a whole. Although never complete, ESM tuning involves adjustments toward both process-level knowledge and emergent (i.e., observed) behaviour. Schmidt et al. (2017) acknowledge a lack of consensus on which type of adjustment is paramount, but fundamentally, both may be required if they are complementary (Danielson et al. 2025). Indeed, we can interpret downscaling and bias correction as the corresponding, complementary forms of tuning that are employed after numerical simulations are provided. The former is endorsed as part of the CMIP6 effort (CORDEX; Eyring et al. 2016) because model resolution is always limited, but regarding bias correction and emergent behaviour, it is also well known that CMIP6 models are not yet sufficiently constrained by observations to perform high resolution impact studies (e.g., Drenkard et al. 2022). Thus, an offline calibration of CMIP6 simulations to a high resolution reanalysis is a relatively low-cost effort a) to parameterize observational constraints during the historical period, and b) to apply these fixed constraints to CMIP6 projections to 2100. Although data files may be large, low-cost refers to a CPU-based statistical downscaling and bias correction that can be performed on a conventional workstation. Neural networks are employed for their flexibility (e.g., it can be shown that they do not distinguish between statistical downscaling and bias correction) and we refer to this calibration as “AI mapping.”

2.1 Datasets

(1) CMIP6 Historical Simulations and Projections

The Sixth Phase of the Coupled Model Intercomparison Project (CMIP6) was organized by the World Climate Research Programme (WCRP) (Eyring et al., 2016). Numerous modelling groups provided historical simulations with observed forcing and ensemble projections to 2100 for different forcing scenarios under the ScenarioMIP experiment. For each climate scenario, Z.

Wang et al. (2024) examined an ensemble member provided by each of 22 modelling groups from the Earth System Grid Federation (ESGF; https://esgf-node.llnl.gov/search/cmip6). Here, we employ the same simulations from each of four Shared Socio-economic Pathway (SSP) scenarios SSP1-2.6, SSP2-4.5, SSP3-7.0, and SSP5-8.5, whose forcing we characterize as:

- **Low: SSP1-2.6**: Radiative forcing reaches a level of 2.6 W/m² by 2100.
- **Intermediate: SSP2-4.5**: Radiative forcing reaches a level of 4.5 W/m² by 2100, representing the medium range of plausible future pathways.
- **High: SSP3-7.0**: Radiative forcing reaches a level of 7.0 W/m² by 2100, representing the medium-to-high end of plausible future pathways.
- **Very High: SSP5-8.5**: Radiative forcing reaches a level of 8.5 W/m² by 2100, representing the upper boundary of the range of scenarios.

By way of radiative forcing, emissions reduction strategies or average global emissions are seen as the causal drivers of outcomes in each scenario. Further details of these 22 ESMs are given by Z. Wang et al. (2024).

(2) GLORYS12 Reanalysis

GLORYS12 (version 1) is a global, eddy-resolving, physical ocean and sea ice reanalysis at 1/12-degree resolution covering the 1993-present altimetry period. A reduced-order Kalman filter is used to assimilate ocean observations, including altimeter sea level anomalies, satellite sea surface temperature, and sea ice concentration, as well as *in situ* temperature and salinity profiles (Lellouche et al. 2021, Mercator Océan International 2022). Numerous studies highlight the spatiotemporal coverage and resolution that is provided. For the MPAs of Fig. 1, McKee et al. (2023) found that GLORYS12 bottom temperature is comparable to *in situ* observations and a monthly gridded analysis. To the north of these MPAs, previous versions of GLORYS were consistent with observed flows along the Labrador Shelf (Wang and Greenan 2013) and Andres et al. (2024) employed GLORYS12 in lieu of sparse observations to document the downstream movement of the cold intermediate layer. Along the US east coast, eight reanalyses are examined by Castillo-Trujillo et al. (2023), who found that GLORYS12 captures the Gulf Stream position and variance well, and was consistent with altimetric observations (as expected). As in McKee et al. (2023), they also confirmed that GLORYS12 is consistent with observations at depth, in part because depth itself is well represented at high resolution.

Observational consistency is aided by adjustments that are applied to the *forcing and predictive* components of GLORYS12 (Lellouche et al. 2021). Specifically, precipitation and radiative fluxes are adjusted toward satellite observations and model prognostic tendencies are nudged to reduce large scale model-observation differences in temperature and salinity, as given by a variational (3DVar) analysis. In principle, emergent (observed) behaviour may be used to constrain the *input (forcing), predictions, and output* of any model (e.g., Danielson et al. 2025). The impetus for using GLORYS12 as a calibration reference is thus partly owing to constraints

that can be said to apply equally to GLORYS12 and CMIP6 models, even if it is only adjustments to CMIP6 ocean model *output* that are considered here.

2.2 Methodology

We treat each neural network in this study as a spatially local parameterization that maps CMIP6 to GLORYS12. With 39 free parameters, each network is flexible and easy to train, but its fixed structure is ad hoc, so trained weights at individual nodes are not easy to associate with specific physical processes. The same neural network calibration is performed for each of six variables: sea surface temperature (SST), bottom temperature (BT), sea surface salinity (SSS), bottom salinity (BS), mixed layer depth (MLD), and bottom current speed (BCS). A total of 22 CMIP6 models are employed under four SSP climate scenarios: SSP1-2.6, SSP2-4.5, SSP3-7.0, and SSP5-8.5. Ensemble averages of all the CMIP6 models were used to provide a consensus of future projections, in part to reduce uncertainties and improve predictive skill (Loder et al. 2015, Z. Wang et al. 2024). The model resolutions of CMIP6 are coarse (mostly ~100 km), whereas the GLORYS12 has a resolution of ~8 km. The processing steps are:

Step 1: Interpolate monthly data for the 22 CMIP6 model solutions onto the GLORYS12 grid.

Step 2: Calculate monthly climatologies of GLORYS12 and the 22 CMIP6 models for the period 1993-2014.

Step 3: Apply an initial bias correction to the CMIP6 model solutions using two methods:

a. For mixed layer depth and bottom currents, the correction factor is determined by the ratio of GLORYS12 to the CMIP6 model from historical simulations. This correction is then applied to the CMIP6 scenario simulations.

b. For other variables, the monthly anomalies for each CMIP6 model are calculated by subtracting the model's monthly climatology. These anomalies are then added to the GLORYS12 monthly climatology to produce a preliminary bias-corrected version of the CMIP6 model output.

Step 4: Apply a neural network to downscale and bias-correct the monthly CMIP6 model data. One neural network is trained for every model (22), variable (6), and gridbox, where the Gully (Fig. 2) has 9x11 gridboxes. Each neural network is defined by 39 parameters (i.e., 3 nodes for input and output, with a four-node hidden layer). Parameters are trained (Innes et al. 2024) using historical data (1993-2014) with CMIP model data as input and GLORYS data as output (the three variables are monthly, centered one-year, and multiyear one-month averages). In turn, the trained neural networks are applied to raw CMIP model data for 2015-2099. Spatial structure that is present in GLORYS is thus introduced, but climate trends in the original CMIP data are preserved (Fig. 2). Following Maraun (2016), trends are determined by the CMIP models, even at high resolution (e.g., CMIP trends are essentially unchanged in Fig. 2).

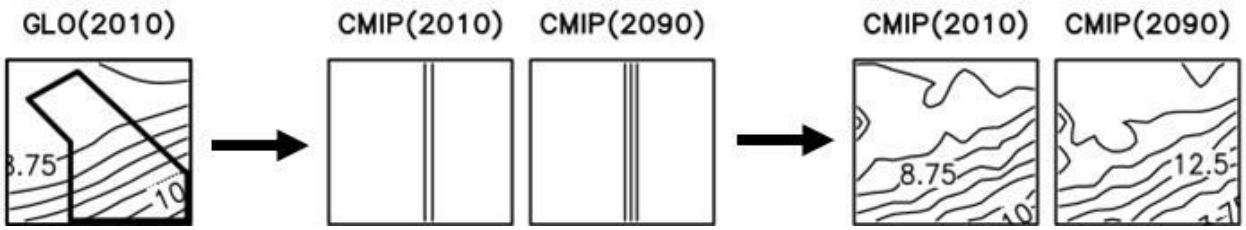

Figure 2: An example of improving SST in the Gully MPA for a representative CMIP6 model. The left panel is GLORYS12 data, center panels are uncalibrated CMIP6 data (i.e., an east-west gradient), and right panels are calibrated CMIP data with trends maintained from the center panel. Each panel is a 20-year average centered on 2000-2020 or 2080-2100, and contours are at 0.25°C intervals.

Step 5: Calculate bi-decadal means and climatologies for Period 1 (P1: 2020-2039), Period 2 (P2: 2040-2059), Period 3 (P3: 2060-2079), and Period 4 (P4: 2080-2099) for the investigated variables.

3. Results and Discussion

In this section, we present the results of Steps 1-5, focusing on how future projections differ from the current conditions, represented by the GLORYS12 hindcast. These differences are assessed using bi-decadal means. While MLD and bottom current speed are not depicted in the figures, analysis of these variables was still conducted, and the results are shown in the tables in this section.

3.1 The Gully MPA

A variety of species inhabit various layers of the Gully, including those living near the sea surface (e.g., mammals such as the Northern Bottlenose Whale, sharks, tunas, plankton), those found as deep as one km below the surface (e.g., halibut, skates, lanternfish), and those at the ocean floor (e.g., crabs, brittle stars, sea pens, cold-water corals) (The Gully). Changes in oceanographic conditions within the MPA may involve shifts in temperature and salinity that exceed the tolerance limits of some species (Boyce et al. 2022, Lewis et al. 2023, Keen et al. 2024).

A CMIP6 model resolution of 1° (about 12,000 km^2) requires about four cells to cover the Gully MPA region (Fig. 2), and after AI mapping to the GLORYS12 grid (Fig. 3), 99 cells are employed. Figure 3 presents the bi-decadal average surface and bottom temperature and salinity conditions for the Gully MPA during the 2040-2059 period under the SSP2-4.5 climate scenario. Also included is a GLORYS12 climatology (1993-2014). Bar plots in the bottom panels illustrate how each climate scenario deviates from that climatology in 20-year periods (corresponding values are provided in Table 1).

Among projected changes in 20-year average anomalies (Table 1), there is greater agreement among CMIP6 models when AI mapping is compared to the original CMIP6 data (i.e., AI mapping enhances precision; Danielson et al. 2025). SST and BT means stand out relative to their standard deviations, and as expected, warming in most of the 22 CMIP6 models is evident.

Models agree less about changes in the other variables (salinity, MLD, and bottom current), although mean and standard deviation values are fairly consistent across all SSP scenarios and 20-year periods. SST increases by about 1°C from present conditions in P1 with only small or no differences between the different SSPs. However, the largest increase occurs under the SSP5-8.5 scenario in P2 and P4, where SST rises by almost 2°C and 4°C, respectively, above current levels. As projections approach 2100, differences between scenarios become more noticeable, and all but one scenario (SSP1) show a warming trend across all periods. SSP1-2.6 stabilizes by P3 and does not change from P3 to P4.

Bottom temperature (Table 1) follows a similar pattern. There is an increase of under 1°C from present conditions, with minimal differences between scenarios. The largest increase in temperature occurs in SSP5-8.5, with a rise of more than 3°C above present conditions in P4. SSP5-8.5 also leads the way in P2, with the scenario showing an increase of over 1.5°C. After P1, each period becomes warmer than the one before.

In terms of SSS (Table 1), changes are minimal in P1, with little difference between SSP1-2.6 and SSP3-7.0. By P2, SSP5-8.5 shows the largest decrease in salinity, and SSP3-7.0 shows the smallest change. In P3, SSP3-7.0 and SSP5-8.5 experience the largest decrease, and SSP1-2.6 shows the smallest. By P4, SSP5-8.5 shows a decrease of just over 1 PSU compared to current conditions. Across all periods, all scenarios trend toward lower salinity, though the differences between scenarios are small.

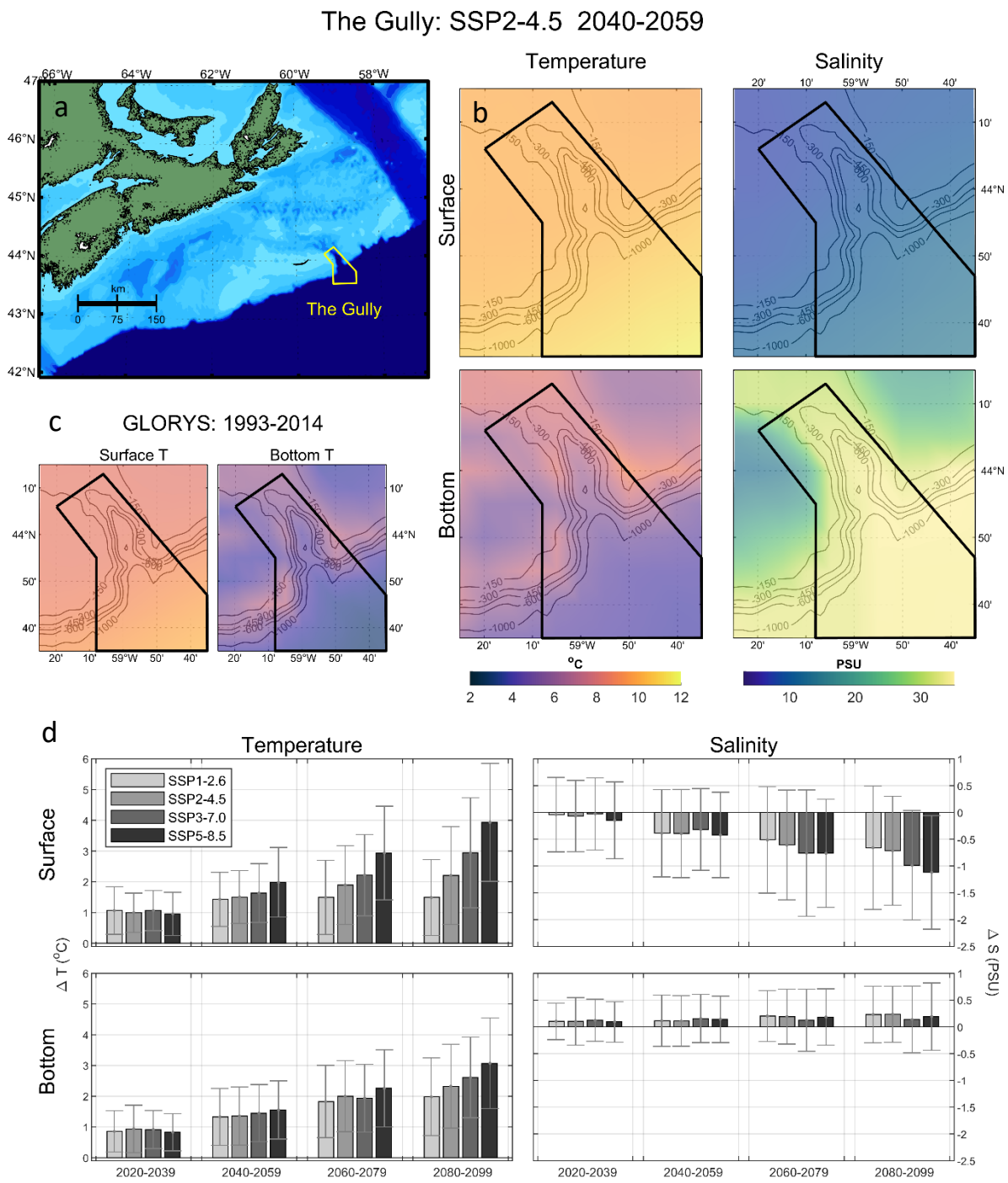

Figure 3: Projected values of temperature and salinity in the Gully MPA. Panels depict a) bathymetry, b) 20-year, multi-model average surface and bottom temperature and salinity for SSP2-4.5 during 2040-2059, c) GLORYS12 climatologies of surface and bottom temperature for 1993-2014, and d) changes in 20-year, multi-model, MPA-average anomalies relative to (c) of surface and bottom temperature and salinity for four SSP scenarios.. The contours in (b) and (c) are bathymetry and the shading is temperature in °C and salinity in PSU, with a colour bar below. Shading in (d) refers to SSPs in the legend at upper left.

Table 1: Projected changes (anomaly ± standard deviation) in oceanic conditions in the Gully MPA from 2020-2099 for four climate scenarios, based on 20-year average periods. P1: 2020-2039; P2: 2040-2059; P3: 2060-2079; P4: 2080-2099. The anomaly is relative to GLORYS12 (1993-2014) and the standard deviation is that of the 22 CMIP6 models.

		P1	P2	P3	P4
SST (°C)	**SSP1-2.6**	1.07 ± 0.77	1.43 ± 0.88	1.49 ± 1.21	1.49 ± 1.23
	SSP2-4.5	0.99 ± 0.64	1.50 ± 0.86	1.89 ± 1.28	2.20 ± 1.59
	SSP3-7.0	1.06 ± 0.65	1.63 ± 0.96	2.22 ± 1.33	2.94 ± 1.79
	SSP5-8.5	0.95 ± 0.70	1.98 ± 1.13	2.93 ± 1.52	3.93 ± 1.92
BT (°C)	**SSP1-2.6**	0.86 ± 0.67	1.33 ± 0.93	1.83 ± 1.18	1.98 ± 1.27
	SSP2-4.5	0.94 ± 0.77	1.35 ± 0.94	2.00 ± 1.16	2.33 ± 1.37
	SSP3-7.0	0.92 ± 0.62	1.45 ± 0.93	1.94 ± 1.11	2.61 ± 1.31
	SSP5-8.5	0.83 ± 0.60	1.56 ± 0.95	2.26 ± 1.26	3.07 ± 1.48
SSS (PSU)	**SSP1-2.6**	-0.04 ± 0.70	-0.39 ± 0.81	-0.51 ± 0.99	-0.66 ± 1.15
	SSP2-4.5	-0.07 ± 0.67	-0.39 ± 0.82	-0.61 ± 1.02	-0.71 ± 1.02
	SSP3-7.0	-0.03 ± 0.67	-0.32 ± 0.76	-0.76 ± 1.18	-0.99 ± 1.02
	SSP5-8.5	-0.15 ± 0.72	-0.42 ± 0.80	-0.76 ± 1.01	-1.12 ± 1.06
BS (PSU)	**SSP1-2.6**	0.10 ± 0.34	0.11 ± 0.48	0.20 ± 0.48	0.23 ± 0.53
	SSP2-4.5	0.10 ± 0.44	0.11 ± 0.47	0.19 ± 0.51	0.23 ± 0.52
	SSP3-7.0	0.12 ± 0.39	0.15 ± 0.45	0.12 ± 0.58	0.14 ± 0.62
	SSP5-8.5	0.09 ± 0.38	0.14 ± 0.43	0.18 ± 0.52	0.19 ± 0.63
MLD (m)	**SSP1-2.6**	-0.68 ± 1.04	-1.37 ± 1.75	-1.45 ± 1.81	-1.27 ± 1.78
	SSP2-4.5	-0.69 ± 1.22	-1.31 ± 1.89	-1.73 ± 2.39	-1.76 ± 1.61
	SSP3-7.0	-0.87 ± 1.42	-1.63 ± 1.66	-2.18 ± 1.88	-2.44 ± 1.68
	SSP5-8.5	-0.88 ± 1.46	-1.83 ± 1.56	-2.26 ± 1.77	-2.81 ± 1.92
Bottom Current Speed (m/s)	**SSP1-2.6**	-0.004 ± 0.012	-0.007 ± 0.013	-0.007 ± 0.015	-0.005 ± 0.014
	SSP2-4.5	-0.003 ± 0.009	-0.006 ± 0.014	-0.007 ± 0.015	-0.005 ± 0.016
	SSP3-7.0	-0.002 ± 0.011	-0.005 ± 0.013	-0.005 ± 0.016	-0.006 ± 0.016
	SSP5-8.5	-0.004 ± 0.010	-0.006 ± 0.015	-0.006 ± 0.018	-0.007 ± 0.018

Bottom salinity (Table 1) remains relatively stable across all periods, with a small increase in P3 and P4. This is likely due to opposing trends in deeper and shallower areas of the ocean, with deeper regions becoming saltier and shallower areas becoming fresher, leading to small changes in the MPA as a whole. SSP1-2.6 and SSP2-4.5 have the largest changes overall in P4, at over 0.2 PSU.

For MLD (Table 1), the smallest change occurs in P1, with SSP1-2.6 showing the least change. Changes become more pronounced in time, with the greatest increase occurring in SSP5-8.5 during P4, when the MLD is more than 2.5 meters shallower than current conditions. The greatest change in P2 also occurs under SSP5-8.5, with the MLD decreasing by more than 1.5 meters. SSP1-2.6 shows a decrease in MLD through P1 to P3, followed by a slight increase in P4, similar to the SST trend under SSP1. In P2, SSP2-4.5 has the smallest change at just over 1.3 m. SSP3-7.0 and SSP5-8.5 both show a steady increase in MLD across the periods.

Finally, the bottom current speed (Table 1) remains relatively stable throughout all periods and scenarios, showing minimal change.

3.2 Laurentian Channel MPA

The Laurentian Channel is a vital habitat for various species, including the black dogfish, and porbeagle and basking sharks. Additionally, two species-at-risk have been found in the area: the northern wolffish and the leatherback sea turtle. The region also boasts the highest concentration of sea pens found anywhere in the entire Newfoundland and Labrador Shelves Bioregion (Laurentian Channel).

A CMIP6 model resolution of 1° requires only about twelve cells to cover the Laurentian Channel MPA, and after AI mapping to GLORYS12 resolution (Fig. 4), 952 cells are employed. This enhanced resolution reveals much greater detail, particularly for BT and BS. Figure 4 also displays the bi-decadal average surface and bottom temperature and salinity conditions for the Laurentian Channel MPA during the 2040-2059 period, based on the SSP2-4.5 climate scenario. For comparison, model data from GLORYS12 representing current conditions (1993-2014) is included. The bar plots in the bottom panel show how each climate scenario deviates from current conditions over the 20-year periods, with corresponding values provided in Table 2.

As shown in Table 2, SST shows a change of approximately 1°C across all scenarios, with SSP1-2.6 having the greatest amount of change. The largest increase in SST occurs under the SSP5-8.5 scenario in P4, with a rise of over 4.5°C above current climatological levels. In P2, SSP5-8.5 also exhibits the most significant change, being the only scenario with an increase of more than 2°C.

Bottom temperature (Table 2) also shows the greatest amount of change in P1 under SSP1-2.6 at more than 1.8°C. The most notable increase happens in SSP5-8.5, where the temperature rises by more than 5.8°C above present state levels in P4. SSP5-8.5 also shows the largest increase in P2 and P3 at more than 3.2°C and 4.5°C, respectively. In P2, SSP2-4.5 has the second largest increase in temperature at just under 3°C.

Sea surface salinity (Table 2) shows a change of around -0.2 PSU in P1, with minimal difference between the scenarios. In P2, SSP5-8.5 shows the largest decline in salinity, followed by SSP1-2.6 with both scenarios projecting a change of more than -0.4 PSU. SSP5-8.5 demonstrates the most significant decrease in both P3 and P4, with the greatest drop occurring in P4, around -1.1 PSU. Throughout P3 and P4, SSP1-2.6 exhibits the least amount of change, while the decrease in salinity intensifies across the other SSPs, reaching its peak in SSP5-8.5. In all periods, all scenarios tend to show a decline in salinity.

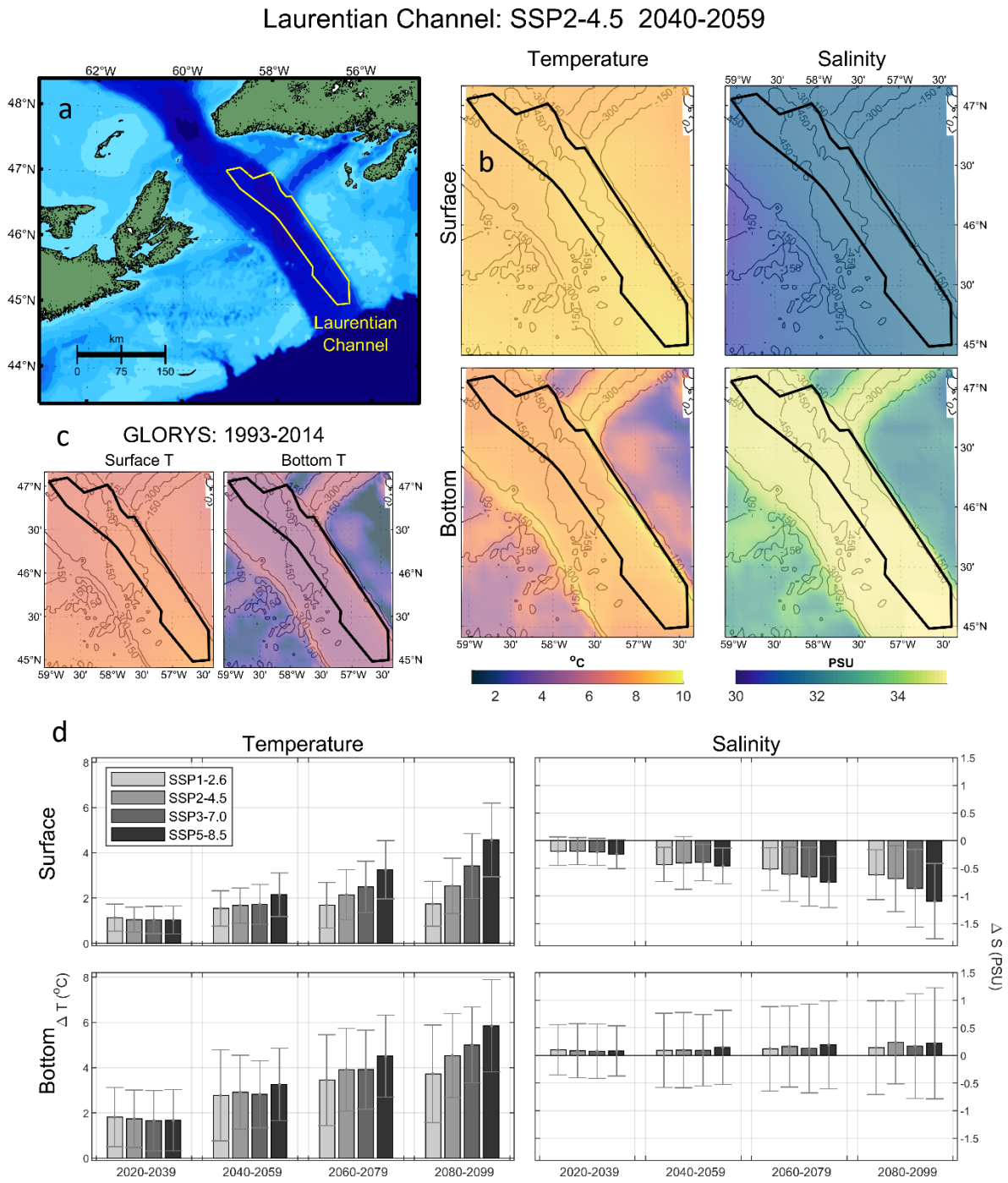

Figure 4: Projected values of temperature and salinity as in Fig. 3, but for the Laurentian Channel MPA.

Table 2: Projected 20-year average changes as in Table 1, but for the Laurentian Channel MPA.

		P1	P2	P3	P4
SST (°C)	**SSP1-2.6**	1.13 ± 0.60	1.54 ± 0.78	1.68 ± 1.00	1.74 ± 0.99
	SSP2-4.5	1.04 ± 0.56	1.67 ± 0.78	2.15 ± 1.11	2.54 ± 1.22
	SSP3-7.0	1.04 ± 0.60	1.72 ± 0.88	2.49 ± 1.14	3.42 ± 1.43
	SSP5-8.5	1.04 ± 0.62	2.15 ± 0.96	3.26 ± 1.29	4.57 ± 1.63
BT (°C)	**SSP1-2.6**	1.81 ± 1.31	2.77 ± 2.01	3.45 ± 2.00	3.72 ± 2.16
	SSP2-4.5	1.74 ± 1.27	2.92 ± 1.64	3.91 ± 1.83	4.53 ± 1.85
	SSP3-7.0	1.66 ± 1.33	2.82 ± 1.48	3.92 ± 1.74	5.00 ± 1.68
	SSP5-8.5	1.67 ± 1.35	3.26 ± 1.60	4.51 ± 1.81	5.85 ± 2.04
SSS (PSU)	**SSP1-2.6**	-0.19 ± 0.26	-0.43 ± 0.31	-0.52 ± 0.39	-0.62 ± 0.45
	SSP2-4.5	-0.19 ± 0.24	-0.40 ± 0.48	-0.61 ± 0.49	-0.69 ± 0.60
	SSP3-7.0	-0.21 ± 0.24	-0.39 ± 0.33	-0.65 ± 0.53	-0.86 ± 0.70
	SSP5-8.5	-0.25 ± 0.26	-0.46 ± 0.32	-0.75 ± 0.46	-1.10 ± 0.68
BS (PSU)	**SSP1-2.6**	0.10 ± 0.45	0.09 ± 0.67	0.12 ± 0.76	0.14 ± 0.85
	SSP2-4.5	0.09 ± 0.49	0.10 ± 0.68	0.16 ± 0.74	0.24 ± 0.75
	SSP3-7.0	0.08 ± 0.49	0.09 ± 0.65	0.13 ± 0.80	0.17 ± 0.95
	SSP5-8.5	0.08 ± 0.45	0.15 ± 0.67	0.19 ± 0.80	0.22 ± 1.00
MLD (m)	**SSP1-2.6**	-0.64 ± 0.77	-0.94 ± 1.36	-0.96 ± 1.51	-1.11 ± 1.56
	SSP2-4.5	-0.54 ± 0.88	-0.87 ± 1.40	-1.24 ± 1.68	-1.55 ± 1.90
	SSP3-7.0	-0.63 ± 0.94	-1.03 ± 1.43	-1.69 ± 1.70	-2.33 ± 1.80
	SSP5-8.5	-0.61 ± 0.81	-1.41 ± 1.35	-2.13 ± 1.85	-2.92 ± 2.08
Bottom Current Speed (m/s)	**SSP1-2.6**	-0.001 ± 0.002	-0.001 ± 0.003	-0.002 ± 0.003	-0.002 ± 0.003
	SSP2-4.5	-0.001 ± 0.002	-0.001 ± 0.003	-0.001 ± 0.003	-0.002 ± 0.003
	SSP3-7.0	-0.001 ± 0.002	-0.001 ± 0.002	-0.001 ± 0.003	-0.002 ± 0.003
	SSP5-8.5	-0.001 ± 0.002	-0.002 ± 0.003	-0.002 ± 0.003	-0.002 ± 0.003

In contrast, BS (Table 2) increases across all SSP scenarios, initially with the exception of SSP1-2.6. In P1, there is minimal change compared to present conditions. In P2, SSP5-8.5 shows a small increase of around 0.15 PSU. SSP5-8.5 has the greatest change in P3 with an increase of just under 0.2 PSU, and in P4, SSP2-4.5 has the largest increase, followed closely by SSP5-8.5 with changes that are both above 0.2 PSU. Mixed layer depth (Table 2) changes by more than -0.5 m across all scenarios in P1. In P2, SSP2-4.5 changes least, by less than -0.9 m, while SSP5-8.5 experiences the largest drop, exceeding -1.4 m. In P3 and P4, changes in MLD increase across all scenarios, with the least change in SSP1-2.6 and the most in SSP5-8.5. The largest reduction occurs in P4 under SSP5-8.5, approaching -3 m. Throughout all periods, all scenarios show a trend toward shallower mixed layers. Finally, bottom current speed (Table 2) remains stable across all periods and scenarios, with negligible change observed.

3.3 St. Anns Bank MPA

Endangered and threatened species that reside in the St. Anns Bank MPA include leatherback turtles, Atlantic wolffish, Atlantic cod, and redfish. This is also an important habitat for white hake, witch flounder, and a variety of sponges, corals, and sea pens (St. Anns Bank).

AI mapping employs 170 cells to cover this MPA, which also exhibits a large annual temperature range (Appendix). SST changes by around 1°C in P1, with SSP1-2.6 seeing the largest change. SSP1-2.6 shows the least change in P2-P4, while SSP5-8.5 exhibits the most significant change in these periods. In P2, the least change is seen in SSP1-2.6, with an increase of over 1.6°C, while the largest change occurs under SSP5-8.5 in P4, with a rise of more than 4.8°C. Across all SSPs, SST is again warmer at the end of the century.

Bottom temperature (Table 3) also has SSP1-2.6 projecting the largest change in P1, more than 1.4°C. Bottom temperature changes follow a similar pattern to SST, with the most significant increases occurring under SSP5-8.5 and the smallest under SSP1-2.6. In P4, the bottom temperature increases by over 5°C under SSP5-8.5. In P2, the largest increase occurs under SSP5-8.5, with the temperature rising more than 3.2°C, while SSP2-4.5 and SSP3-7.0 have smaller increases of about 2°C.

Sea surface salinity (Table 3) decreases by more than -0.2 PSU in P1, with the greatest drop occurring under SSP5-8.5 and the least under SSP1-2.6. In P2, SSP5-8.5 has the largest decrease of more than -0.4 PSU, while SSP1-2.6 remains almost unchanged. In P3, SSP5-8.5 shows the largest decrease of -0.6 PSU, and in P4, the largest decrease reaches almost -1.2 PSU. All scenarios show a decreasing trend in SSS across all periods.

Bottom salinity (Table 3) shows minimal change in P1 for all SSPs. SSP5-8.5 shows the greatest change across P2-P4, and SSP1-2.6 shows the least. The greatest change in PSU by the end of the century is in P4 with SSP5-8.5, with an increase of more than 0.2 PSU. All SSPs are more saline at the end of the century.

Mixed layer depth (Table 3) under SSP1-2.6 remains relatively stable, with a change of around -0.33 m in P1-P3, and then increases slightly to around -0.25 m in P4. SSP1-2.6 also has the least change across periods P2-P4. SSP5-8.5 shows the largest change across P2-P4, with the most significant reduction in MLD occurring in P4, at around -1.75 m. The greatest decrease in MLD in P2 is observed under SSP5-8.5, with a reduction of just under -0.75 m. All scenarios trend towards a shallower MLD by 2100. Bottom current speed remains unchanged throughout all periods and scenarios, showing no trend.

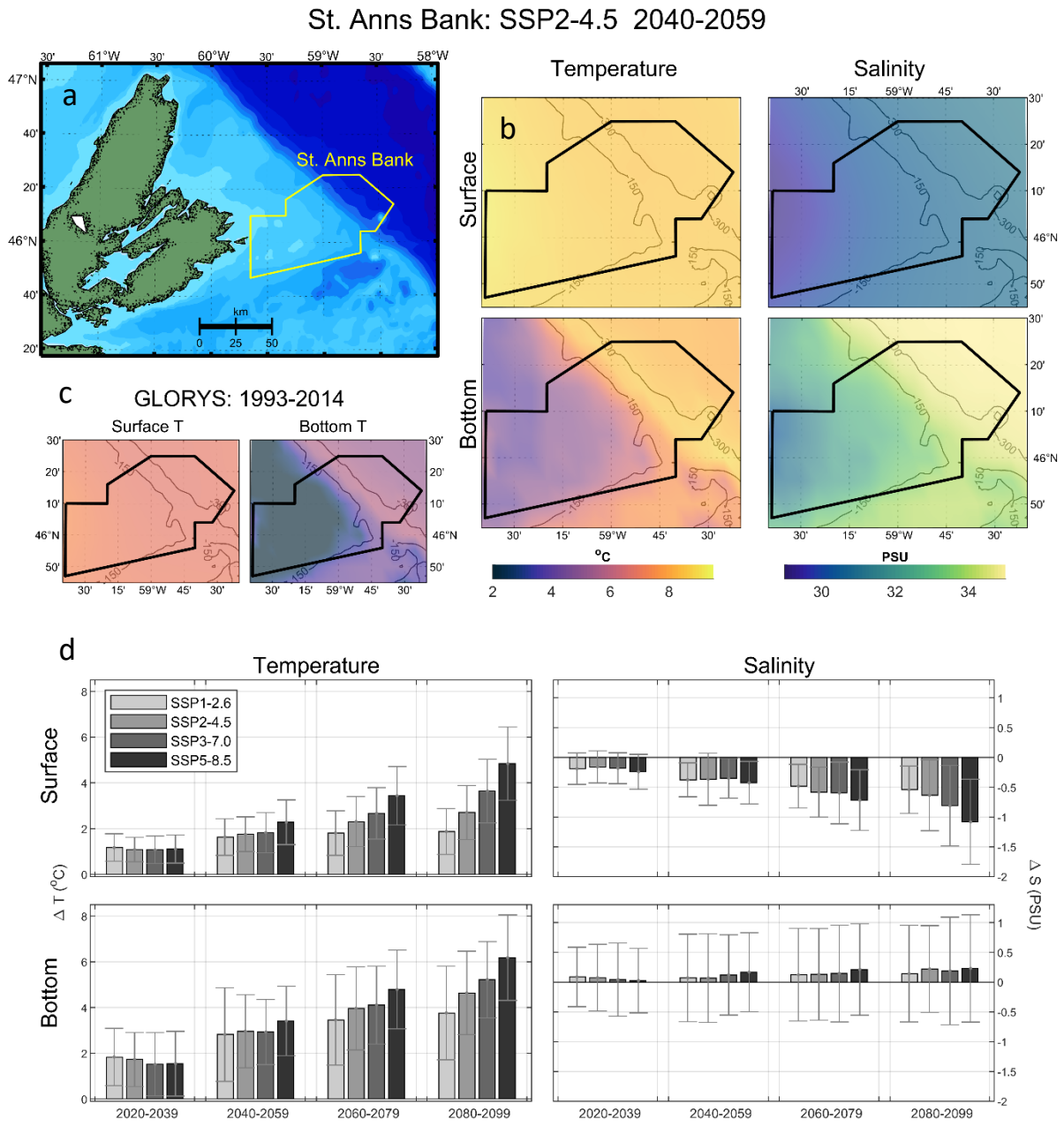

Figure 5: Projected values of temperature and salinity as in Fig. 3, but for the St. Anns Bank MPA.

Table 3: Projected 20-year average changes as in Table 1, but for the St. Anns Bank MPA.

		P1	P2	P3	P4
SST (°C)	**SSP1-2.6**	1.17 ± 0.60	1.63 ± 0.80	1.81 ± 0.98	1.88 ± 1.00
	SSP2-4.5	1.09 ± 0.53	1.75 ± 0.76	2.30 ± 1.09	2.71 ± 1.18
	SSP3-7.0	1.08 ± 0.60	1.82 ± 0.88	2.66 ± 1.12	3.65 ± 1.39
	SSP5-8.5	1.10 ± 0.61	2.28 ± 0.97	3.44 ± 1.27	4.84 ± 1.61
BT (°C)	**SSP1-2.6**	1.84 ± 1.25	2.82 ± 2.05	3.46 ± 1.98	3.76 ± 2.05
	SSP2-4.5	1.73 ± 1.18	2.96 ± 1.60	3.96 ± 1.82	4.64 ± 1.83
	SSP3-7.0	1.52 ± 1.38	2.93 ± 1.42	4.11 ± 1.70	5.22 ± 1.66
	SSP5-8.5	1.55 ± 1.41	3.41 ± 1.52	4.79 ± 1.72	6.18 ± 1.86
SSS (PSU)	**SSP1-2.6**	-0.19 ± 0.26	-0.37 ± 0.29	-0.48 ± 0.36	-0.54 ± 0.40
	SSP2-4.5	-0.16 ± 0.27	-0.37 ± 0.44	-0.58 ± 0.42	-0.63 ± 0.60
	SSP3-7.0	-0.18 ± 0.26	-0.35 ± 0.33	-0.59 ± 0.52	-0.81 ± 0.68
	SSP5-8.5	-0.24 ± 0.29	-0.42 ± 0.36	-0.72 ± 0.51	-1.08 ± 0.72
BS (PSU)	**SSP1-2.6**	0.09 ± 0.50	0.07 ± 0.74	0.12 ± 0.78	0.14 ± 0.81
	SSP2-4.5	0.07 ± 0.56	0.07 ± 0.74	0.13 ± 0.77	0.22 ± 0.73
	SSP3-7.0	0.04 ± 0.61	0.12 ± 0.67	0.14 ± 0.81	0.19 ± 0.90
	SSP5-8.5	0.03 ± 0.54	0.17 ± 0.66	0.21 ± 0.77	0.23 ± 0.90
MLD (m)	**SSP1-2.6**	-0.32 ± 0.65	-0.33 ± 1.23	-0.35 ± 1.25	-0.24 ± 1.53
	SSP2-4.5	-0.20 ± 0.80	-0.36 ± 1.22	-0.49 ± 1.56	-0.67 ± 1.59
	SSP3-7.0	-0.33 ± 0.89	-0.57 ± 1.20	-0.84 ± 1.39	-1.24 ± 1.62
	SSP5-8.5	-0.24 ± 0.78	-0.74 ± 1.25	-1.15 ± 1.58	-1.75 ± 1.63
Bottom Current Speed (m/s)	**SSP1-2.6**	-0.001 ± 0.002	-0.002 ± 0.003	-0.002 ± 0.003	-0.002 ± 0.003
	SSP2-4.5	-0.001 ± 0.002	-0.001 ± 0.003	-0.001 ± 0.002	-0.002 ± 0.003
	SSP3-7.0	-0.001 ± 0.002	-0.001 ± 0.002	-0.001 ± 0.003	-0.002 ± 0.003
	SSP5-8.5	-0.001 ± 0.002	-0.002 ± 0.003	-0.002 ± 0.003	-0.002 ± 0.003

3.4 Basin Head MPA

The Basin Head MPA was established to protect the Basin Head Irish moss (Chondrus crispus), a species of moss that may be endemic to this MPA (Basin Head). Covering just nine square kilometers, this MPA fits within part of a larger climate model grid cell, and even after AI mapping, there is almost no spatial variation (two grid cells) in future climate scenario projections. Data for this MPA are thus shown using line plots rather than colour maps.

Figure 6b shows annual average conditions for SST and BT. Different SSPs reveal little variation from 2015 until around 2040, after which SSP5-8.5 begins to diverge. By the century's end, SSP1-2.6 captures the lowest temperatures and SSP5-8.5 the highest. In terms of salinity, the divergence among SSPs is less apparent, although SSP5-8.5 has the lowest salinity (both SSS and BS) by 2100.

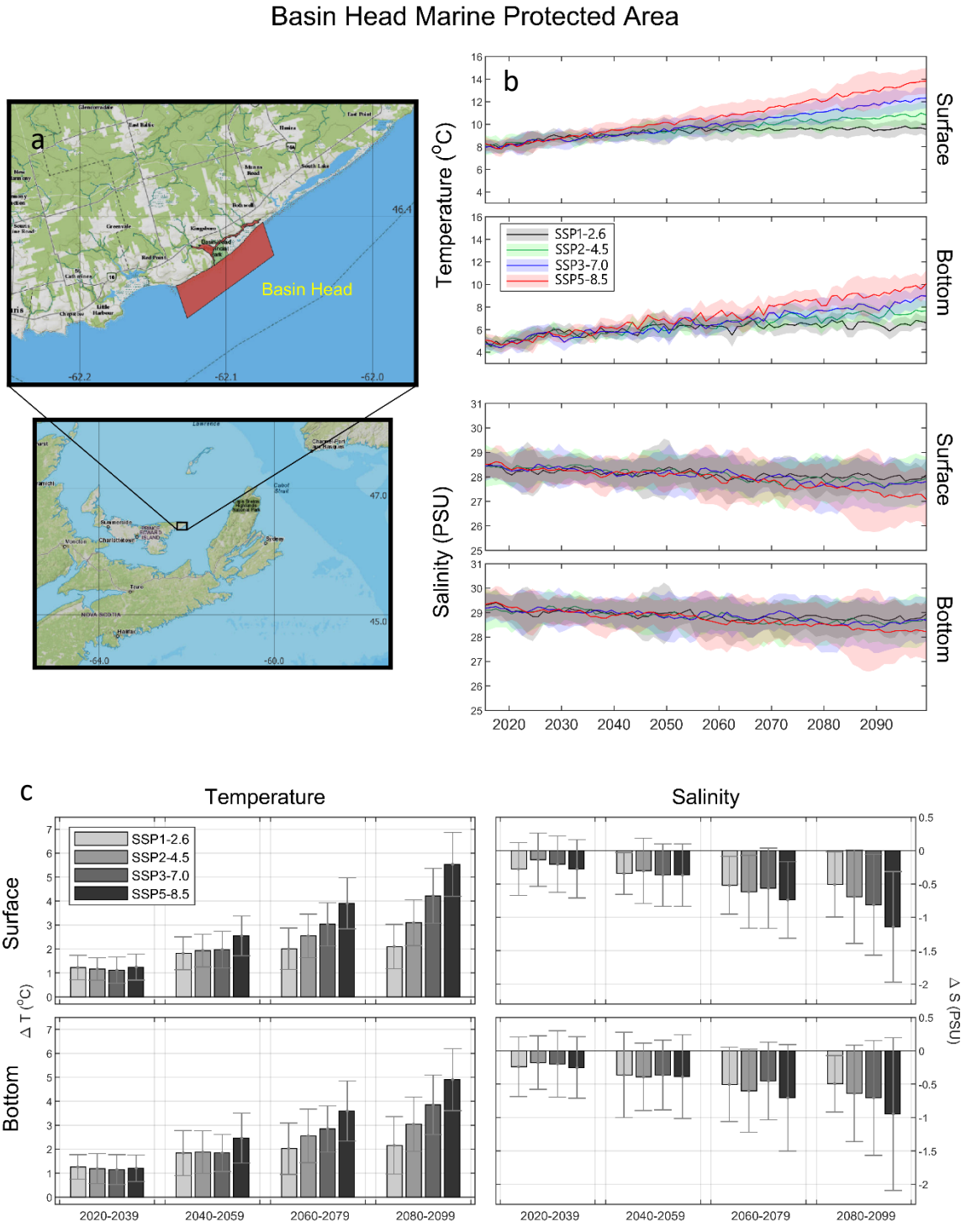

Figure 6: Projected values of temperature and salinity in the Basin Head MPA. Panels depict a) location, b) timeseries of annual average surface and bottom temperature and salinity for the multi-model average (lines) and 22-model standard deviation (shading), and c) changes in 20-year, multi-model, MPA-average anomalies relative to the 1993-2014 GLORYS12 climatologies of surface and bottom temperature and salinity for four SSP scenarios. The shading in (b) and (c) refer to SSPs in legends at upper left.

Table 4: Projected 20-year average changes as in Table 1, but for the Basin Head MPA.

		P1	P2	P3	P4
SST (°C)	**SSP1-2.6**	1.22 ± 0.51	1.82 ± 0.69	2.01 ± 0.87	2.10 ± 0.92
	SSP2-4.5	1.16 ± 0.47	1.93 ± 0.69	2.55 ± 0.91	3.09 ± 0.95
	SSP3-7.0	1.12 ± 0.55	1.98 ± 0.77	3.03 ± 0.90	4.22 ± 1.15
	SSP5-8.5	1.25 ± 0.54	2.55 ± 0.83	3.91 ± 1.07	5.53 ± 1.34
BT (°C)	**SSP1-2.6**	1.26 ± 0.51	1.84 ± 0.94	2.02 ± 1.07	2.16 ± 1.20
	SSP2-4.5	1.19 ± 0.62	1.88 ± 0.89	2.56 ± 1.12	3.04 ± 1.14
	SSP3-7.0	1.15 ± 0.62	1.85 ± 0.77	2.85 ± 0.97	3.85 ± 1.25
	SSP5-8.5	1.21 ± 0.56	2.47 ± 1.04	3.59 ± 1.26	4.90 ± 1.30
SSS (PSU)	**SSP1-2.6**	-0.28 ± 0.40	-0.34 ± 0.31	-0.52 ± 0.43	-0.51 ± 0.49
	SSP2-4.5	-0.14 ± 0.40	-0.30 ± 0.49	-0.62 ± 0.55	-0.69 ± 0.70
	SSP3-7.0	-0.20 ± 0.42	-0.37 ± 0.47	-0.56 ± 0.60	-0.81 ± 0.75
	SSP5-8.5	-0.27 ± 0.44	-0.37 ± 0.47	-0.74 ± 0.57	-1.14 ± 0.83
BS (PSU)	**SSP1-2.6**	-0.24 ± 0.45	-0.36 ± 0.64	-0.50 ± 0.56	-0.49 ± 0.42
	SSP2-4.5	-0.18 ± 0.40	-0.39 ± 0.51	-0.60 ± 0.62	-0.64 ± 0.72
	SSP3-7.0	-0.20 ± 0.50	-0.36 ± 0.52	-0.45 ± 0.58	-0.71 ± 0.86
	SSP5-8.5	-0.25 ± 0.46	-0.39 ± 0.63	-0.71 ± 0.80	-0.95 ± 1.15
MLD (m)	**SSP1-2.6**	-0.07 ± 0.38	-0.16 ± 0.61	-0.12 ± 0.71	-0.00 ± 0.82
	SSP2-4.5	-0.08 ± 0.41	-0.06 ± 0.65	-0.12 ± 0.80	-0.22 ± 0.87
	SSP3-7.0	-0.02 ± 0.57	-0.29 ± 0.68	-0.37 ± 0.97	-0.53 ± 1.17
	SSP5-8.5	-0.03 ± 0.62	-0.31 ± 0.88	-0.58 ± 1.07	-0.84 ± 1.22
Bottom Current Speed (m/s)	**SSP1-2.6**	0.000 ± 0.003	0.000 ± 0.004	-0.001 ± 0.004	-0.001 ± 0.005
	SSP2-4.5	0.000 ± 0.002	0.000 ± 0.004	-0.001 ± 0.005	-0.001 ± 0.005
	SSP3-7.0	0.000 ± 0.002	-0.001 ± 0.004	0.000 ± 0.005	-0.001 ± 0.005
	SSP5-8.5	0.000 ± 0.003	-0.001 ± 0.003	-0.002 ± 0.004	-0.002 ± 0.005

As seen in Table 4, P1 SST shows minimal change across all SSPs, with projections remaining fairly consistent at a change of slightly more than 1°C. Again, projections for SSP5-8.5 begin to diverge at around 2040. SSP1-2.6 experiences the least change in the later periods (P2-P4), with a temperature increase of more than 2°C by P4, while SSP5-8.5 shows the most significant change, particularly in P4, with an increase of more than 5.5°C.

Bottom temperature (Table 4) shows SSP1-2.6 displaying the greatest change in P1, followed by the least change in P2-P4. SSP5-8.5 experiences the most significant rise from P2-P4, with values of around 2.5°C in P2 and just under 5°C in P4. Both SST and BT show a trend toward warmer temperatures by the end of the century.

For SSS (Table 4), SSP1-2.6 has the greatest change in P1 at under -0.3 PSU, and SSP2-4.5 the least at around -0.15 PSU. In P2, SSP2-4.5 also has the smallest decrease in salinity, around -0.3 PSU, while SSP3-7.0 and SSP5-8.5 experience a slightly greater decrease of more than -0.35 PSU. In later periods (P3-P4), SSP1-2.6 shows the least amount of change, with a decrease of

just over -0.5 PSU in P3 and P4, while SSP5-8.5 sees the greatest changes, with a decrease of more than -1.0 PSU by the end of the century.

Bottom salinity (Table 4) shows changes of around -0.2 PSU in P1 for all SSPs. In P2, SSP1-2.6 and SSP3-7.0 have the smallest decreases in salinity (about -0.35 PSU), while SSP2-4.5 and SSP5-8.5 have the largest decrease (around -0.4 PSU). By P4, the changes in bottom salinity increase across all SSPs, with SSP1-2.6 showing a decrease of just under -0.5 PSU and SSP5-8.5 showing the largest decrease at just under -1.0 PSU. All SSPs show a trend toward lower salinity by the end of the century.

Mixed Layer Depth (Table 4) shows some divergence across SSPs. In P1 and P2, SSP1-2.6 shows the MLD becoming shallower, and then deeper in P3 to P4, and ending the century at a depth similar to present conditions. In P2, SSP3-7.0 and SSP5-8.5 have similar depths, though SSP5-8.5 has a slightly larger change (just over -0.3 m). In P3, SSP1-2.6 and SSP2-4.5 change the least (~-0.1 m) and SSP5-8.5 the most (under -0.6 m). By P4, SSP2-4.5 to SSP5-8.5 show the MLD becoming shallower, with SSP5-8.5 exhibiting the greatest change of more than -0.8 m. Lastly, bottom current projections show no significant change or trend by the end of the century.3.5 Banc-des-Américains MPA

3.5 Banc-des-Américains MPA

The Banc-des-Américains MPA is regularly visited by blue whales and is home to Atlantic wolffish. Species at risk, such as the Spotted wolffish and Northern wolffish, have been found in the region. Leatherback turtles have also been observed within the MPA as well. This area provides crucial feeding, spawning, shelter, and migration habitats for many of these species (Banc-des-Américains).

AI mapping improves the representation of the Banc-des-Américains MPA by using 42 grid cells (Fig. 7b,c) instead of just a few for most CMIP6 models. As shown in Table 5, SST increases by about 1°C in P1, with all SSP scenarios being fairly similar. SSP1-2.6 experiences the smallest change in P2-P4, while SSP5-8.5 shows the largest changes during these periods. The smallest change in P2 is observed in SSP1-2.6, with an increase of less than 1.8°C, while the largest overall increase occurs under SSP5-8.5 in P4, with a rise of over 5.4°C. Across all SSP scenarios, SST trends warmer by the end of the century.

Bottom temperature (Table 5) does show some variation among the SSPs in P1, with SSP2-4.5 projecting the largest change at under 1.4°C. SSP2-4.5 then shows the smallest change in P2, with an increase of just over 2°C, while SSP5-8.5 exhibits the largest change in P2, with an increase of more than 2.4°C. SSP1-2.6 experiences the smallest changes in P3 and P4, while SSP5-8.5 shows the largest changes in these periods, with the greatest overall change occurring in P4 at more than 5°C. All SSP scenarios trend toward warmer bottom temperatures by the end of the century.

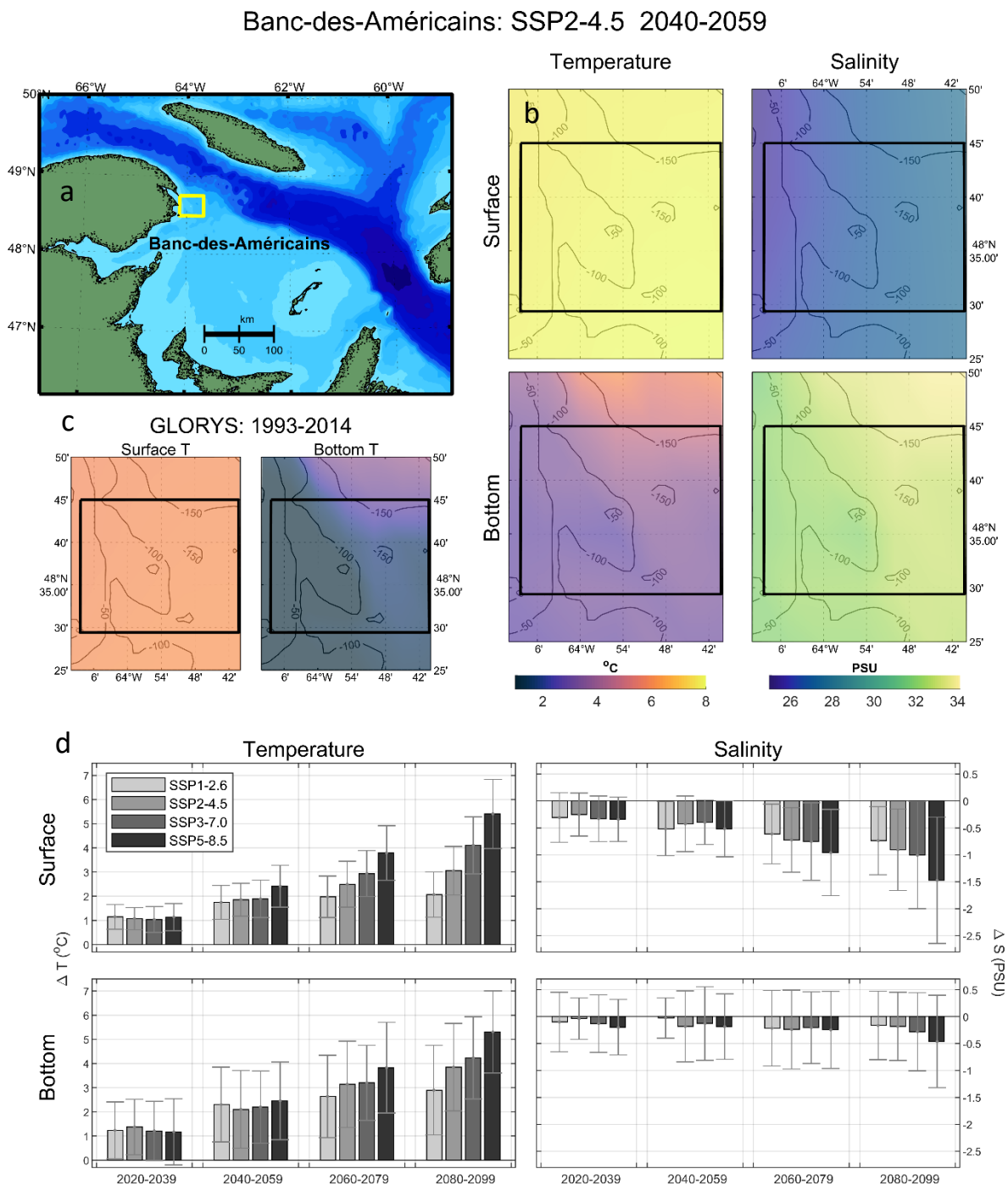

Figure 7: Projected values of temperature and salinity as in Fig. 3, but for the Banc-des-Américains MPA.

Table 5: Projected 20-year average changes as in Table 1, but for the Banc-des-Américains MPA.

		P1	P2	P3	P4
SST (°C)	**SSP1-2.6**	1.15 ± 0.51	1.74 ± 0.70	1.97 ± 0.86	2.07 ± 0.93
	SSP2-4.5	1.07 ± 0.46	1.86 ± 0.68	2.49 ± 0.95	3.05 ± 1.01
	SSP3-7.0	1.03 ± 0.53	1.89 ± 0.77	2.93 ± 0.95	4.10 ± 1.18
	SSP5-8.5	1.14 ± 0.56	2.41 ± 0.87	3.79 ± 1.13	5.41 ± 1.43
BT (°C)	**SSP1-2.6**	1.23 ± 1.18	2.30 ± 1.55	2.64 ± 1.70	2.90 ± 1.85
	SSP2-4.5	1.37 ± 1.15	2.10 ± 1.60	3.14 ± 1.78	3.85 ± 1.81
	SSP3-7.0	1.21 ± 1.22	2.20 ± 1.49	3.20 ± 1.55	4.23 ± 1.70
	SSP5-8.5	1.17 ± 1.37	2.45 ± 1.61	3.82 ± 1.88	5.31 ± 1.70
SSS (PSU)	**SSP1-2.6**	-0.31 ± 0.46	-0.52 ± 0.50	-0.61 ± 0.55	-0.74 ± 0.63
	SSP2-4.5	-0.25 ± 0.40	-0.43 ± 0.52	-0.72 ± 0.60	-0.91 ± 0.76
	SSP3-7.0	-0.33 ± 0.42	-0.40 ± 0.41	-0.75 ± 0.72	-1.01 ± 0.99
	SSP5-8.5	-0.34 ± 0.41	-0.52 ± 0.52	-0.96 ± 0.80	-1.47 ± 1.17
BS (PSU)	**SSP1-2.6**	-0.10 ± 0.55	-0.03 ± 0.37	-0.22 ± 0.70	-0.16 ± 0.64
	SSP2-4.5	-0.04 ± 0.38	-0.18 ± 0.66	-0.24 ± 0.73	-0.18 ± 0.63
	SSP3-7.0	-0.13 ± 0.54	-0.13 ± 0.68	-0.20 ± 0.66	-0.28 ± 0.73
	SSP5-8.5	-0.20 ± 0.52	-0.18 ± 0.61	-0.25 ± 0.72	-0.46 ± 0.86
MLD (m)	**SSP1-2.6**	-0.35 ± 0.68	-0.51 ± 1.04	-0.45 ± 1.00	-0.48 ± 1.10
	SSP2-4.5	-0.37 ± 0.67	-0.44 ± 0.88	-0.55 ± 1.10	-0.77 ± 1.33
	SSP3-7.0	-0.34 ± 0.69	-0.59 ± 0.97	-0.92 ± 1.27	-1.14 ± 1.74
	SSP5-8.5	-0.28 ± 0.75	-0.75 ± 1.13	-1.06 ± 1.57	-1.59 ± 1.88
Bottom Current Speed (m/s)	**SSP1-2.6**	0.000 ± 0.001	0.000 ± 0.001	0.000 ± 0.002	0.001 ± 0.002
	SSP2-4.5	0.000 ± 0.001	0.000 ± 0.001	0.000 ± 0.002	0.000 ± 0.001
	SSP3-7.0	0.000 ± 0.001	0.000 ± 0.001	0.000 ± 0.002	0.000 ± 0.002
	SSP5-8.5	0.000 ± 0.001	0.000 ± 0.001	0.000 ± 0.002	0.000 ± 0.002

For SSS (Table 5), there is a change of around -0.3 PSU, with all SSP scenarios showing similar projections. SSP3-7.0 experiences the smallest change in P2, with a decrease of around -0.4 PSU, while SSP1-2.6 and SSP5-8.5 have the largest changes, with a decrease of over -0.5 PSU. SSP1-2.6 shows the smallest change in both P3 and P4, while SSP5-8.5 has the largest changes in these periods, with the largest overall decrease occurring in P4 under SSP5-8.5, at under -1.5 PSU. All SSP scenarios trend toward lower salinity by the end of the century.

Bottom salinity (Table 5) shows changes of around -0.3 PSU to -0.4 PSU for all SSPs. SSP2-4.5 and SSP5-8.5 exhibit the greatest change in P2 and P3, with a decrease of about -0.2 PSU in P2 and -0.25 PSU in P3. SSP1-2.6 shows almost no change from present conditions in P2, and all SSPs project similar conditions in P3. SSP5-8.5 shows the greatest overall change in P4, with a decrease of just under -0.5 PSU. By the end of the century, all SSPs trend toward less saline conditions.

Mixed layer depth (Table 5) shows a similar trend to the Basin Head MPA, where SSP1-2.6 first trends shallower, then deeper in the second half of the century. SSP5-8.5 has the least amount of change in P1, and the most amount of change in P2-P4, with the greatest overall change in P4

with a change of around -1.5 m. SSP1-2.6 shows the least amount of change in P3 and P4, with a change of under -0.5 m in both P3 and P4. For SSP2-4.5 to SSP5-8.5, the mixed layer depth trends toward becoming shallower by the end of the century. Finally, bottom current speed shows no significant change or trend across any of the periods or SSP scenarios.

3.6 Musquash Estuary MPA

The Musquash Estuary MPA in the Bay of Fundy exists to protect the natural state of the estuary and salt marshes, including the habitat of many birds, fish, mammals, invertebrates, and marine plants (Musquash Estuary). As with the Basin Head MPA, this MPA (7.4 square kilometers) is difficult to capture by CMIP6 models as a portion is inland, and even after AI mapping, is represented by only two grid cells. Thus, annual average conditions are shown as line plots, as for the Basin Head MPA.

The different SSPs in Fig. 8b show little variation from 2015 until around 2040, after which SSP5-8.5 begins to diverge. By century's end, temperature and SSP correspond, with SSP1-2.6 displaying the lowest temperature and SSP5-8.5 the highest. In terms of salinity, the divergence among SSPs is less distinct (except for SSP5-8.5 around 2060), with SSP5-8.5 having the lowest salinity (both SSS and BS) by 2100.

Table 6 shows initial (P1) SST changes of around 1°C, with all SSPs being similar. However, projected changes differ more with time. For instance, SSP1-2.6 changes least during P2 to P4, while SSP5-8.5 shows significant warming, with P2 exceeding 2.2°C. The greatest warming occurs in P4 under SSP5-8.5, with a change of around 4.5°C. All SSPs trend toward warmer temperatures.

Bottom temperature (Table 6) varies among the SSPs during P1, with SSP3-7.0 showing the least change at under 1°C, and SSP5-8.5 the most at around 1.2°C. In P2-P4, SSP5-8.5 projects the greatest temperature increase, while SSP1-2.6 the least. The largest change is projected for P4 under SSP5-8.5, with an increase of just under 5°C. Like SST, all SSPs trend warmer by the end of the century.

Sea surface salinity (Table 6) shows minimal change in P1, with all SSPs being similar. In P2, SSP1-2.6 and SSP3-7.0 show the greatest decrease in salinity, with a reduction of about -0.4 PSU, while SSP2-4.5 shows the least change, at just under -0.3 PSU. In P3 and P4, SSP1-2.6 shows the smallest changes, and SSP5-8.5 the greatest. The reduction in salinity is greatest for P4 under SSP5-8.5, with a decrease of more than -2 PSU, but surface salinity decreases under all SSPs.

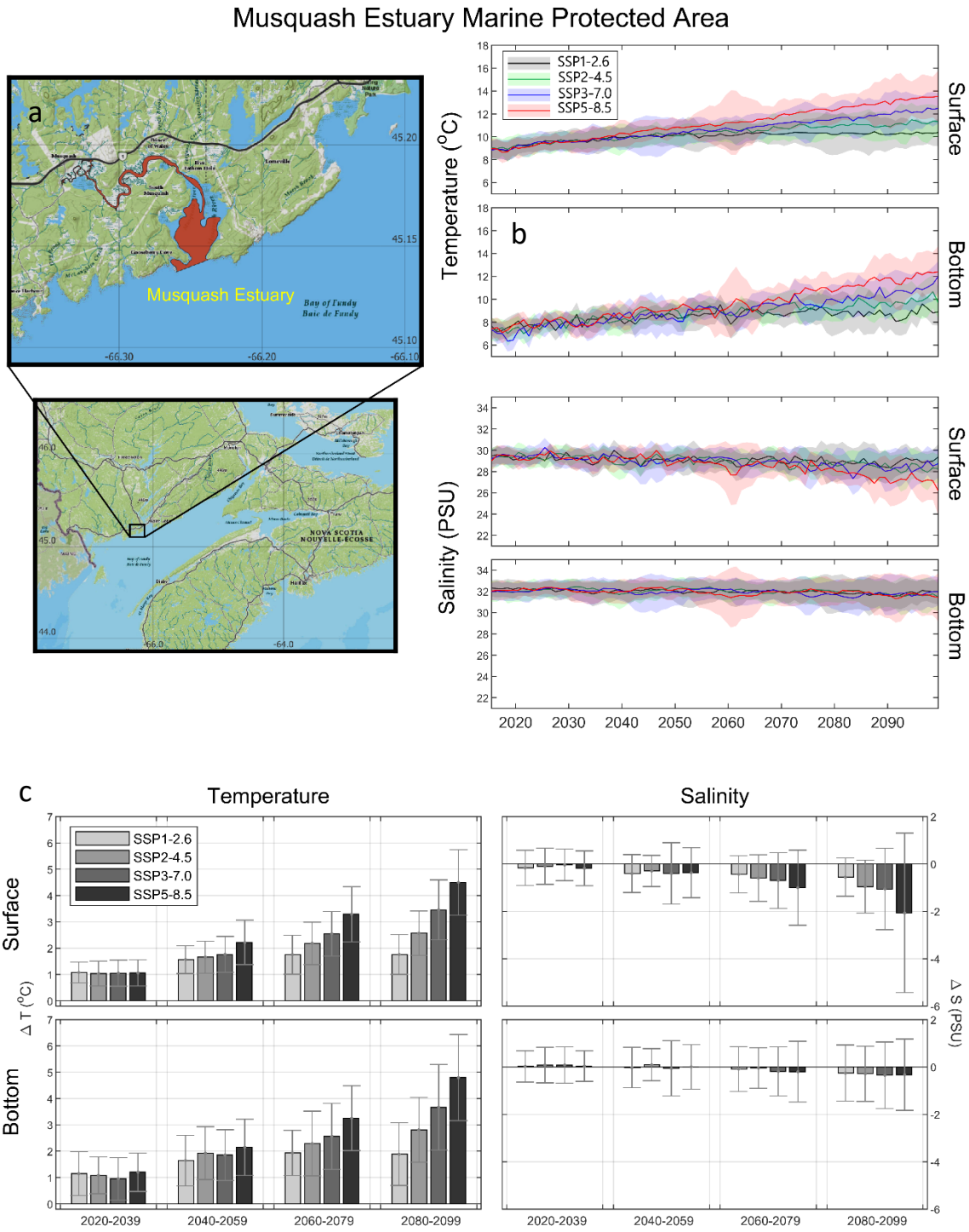

Figure 8: Projected values of temperature and salinity as in Fig. 6, but for the Musquash Estuary MPA.

Table 6: Projected 20-year average changes as in Table 1, but for the Musquash Estuary MPA.

		P1	P2	P3	P4
SST (°C)	**SSP1-2.6**	1.08 ± 0.39	1.57 ± 0.53	1.75 ± 0.74	1.76 ± 0.76
	SSP2-4.5	1.04 ± 0.47	1.66 ± 0.60	2.19 ± 0.81	2.57 ± 0.84
	SSP3-7.0	1.05 ± 0.50	1.76 ± 0.68	2.55 ± 0.85	3.46 ± 1.14
	SSP5-8.5	1.06 ± 0.50	2.22 ± 0.84	3.29 ± 1.05	4.50 ± 1.25
BT (°C)	**SSP1-2.6**	1.15 ± 0.83	1.64 ± 0.96	1.94 ± 0.86	1.89 ± 1.19
	SSP2-4.5	1.08 ± 0.70	1.93 ± 1.01	2.29 ± 1.23	2.81 ± 1.23
	SSP3-7.0	0.95 ± 0.81	1.86 ± 0.97	2.56 ± 1.26	3.67 ± 1.63
	SSP5-8.5	1.20 ± 0.73	2.15 ± 1.07	3.25 ± 1.23	4.80 ± 1.64
SSS (PSU)	**SSP1-2.6**	-0.16 ± 0.74	-0.40 ± 0.80	-0.44 ± 0.79	-0.56 ± 0.81
	SSP2-4.5	-0.10 ± 0.76	-0.29 ± 0.66	-0.59 ± 0.98	-0.96 ± 1.12
	SSP3-7.0	-0.04 ± 0.67	-0.40 ± 1.29	-0.70 ± 1.18	-1.06 ± 1.72
	SSP5-8.5	-0.18 ± 0.73	-0.37 ± 1.05	-1.00 ± 1.59	-2.06 ± 3.36
BS (PSU)	**SSP1-2.6**	0.03 ± 0.66	-0.02 ± 0.85	-0.09 ± 0.94	-0.26 ± 1.19
	SSP2-4.5	0.08 ± 0.75	0.10 ± 0.68	-0.04 ± 0.86	-0.28 ± 1.16
	SSP3-7.0	0.08 ± 0.76	-0.06 ± 1.17	-0.19 ± 1.04	-0.35 ± 1.40
	SSP5-8.5	0.04 ± 0.65	0.00 ± 0.94	-0.20 ± 1.28	-0.33 ± 1.51
MLD (m)	**SSP1-2.6**	-0.49 ± 0.82	-0.69 ± 0.82	-0.65 ± 1.00	-0.74 ± 1.15
	SSP2-4.5	-0.46 ± 0.80	-0.79 ± 1.10	-1.03 ± 1.20	-0.97 ± 1.17
	SSP3-7.0	-0.51 ± 0.77	-0.87 ± 1.22	-1.07 ± 1.33	-1.21 ± 1.73
	SSP5-8.5	-0.59 ± 0.87	-1.05 ± 1.17	-1.42 ± 1.36	-1.46 ± 1.75
Bottom Current Speed (m/s)	**SSP1-2.6**	0.002 ± 0.003	0.003 ± 0.005	0.003 ± 0.005	0.004 ± 0.006
	SSP2-4.5	0.003 ± 0.005	0.002 ± 0.004	0.003 ± 0.005	0.003 ± 0.006
	SSP3-7.0	0.003 ± 0.004	0.003 ± 0.004	0.003 ± 0.005	0.004 ± 0.007
	SSP5-8.5	0.002 ± 0.004	0.003 ± 0.004	0.003 ± 0.005	0.002 ± 0.007

Bottom salinity (Table 6) exhibits minimal change in P1, with the SSPs showing similar projections. In P2, while still similar to present conditions, SSP2-4.5 projects a slight increase in PSU, while SSP1-2.6 and SSP3-7.0 project slight decreases. SSP5-8.5 changes little from present climatological conditions in P2. In P3, more variation is observed, with SSP5-8.5 changing the most (around -0.2 PSU) and SSP2-4.5 the least (just above 0.0 PSU). In P4, there is little variation among the SSPs, but the largest overall change occurs in SSP3-7.0, with a decrease of more than -0.3 PSU. All SSPs trend toward less saline bottom waters.

Mixed layer depth (Table 6) is projected to become shallower by about 0.5 m in P1, with the largest decrease seen under SSP5-8.5. In P2, SSP1-2.6 changes the least (under -0.7 m), while SSP5-8.5 changes the most (over -1 m). This is the same in P4, with SSP5-8.5 approaching -1.5 m. SSP2-4.5 MLD becomes shallower from P1 to P3, and then deeper in P4 (relative to P3). The remaining SSPs indicate a consistent thinning of MLD. Again, bottom current speed shows minimal change across all periods and SSPs.

4. Conclusions

AI mapping, or statistical downscaling and bias correction, is employed to provide ocean conditions at higher resolution within MPAs (Figs. 3-8), and more precise projections of ocean conditions, and where trends in CMIP6 models are essentially unchanged (Danielson et al. 2025). When combined with climate projections from the CMIP6 scenarios, AI mapping can help biologists to assess whether species are at risk of significant changes to their habitat. As expected, the SSP5-8.5 scenario leads to the most significant changes in ocean conditions, but potential shifts in the ecosystem under all scenarios are of interest. The 22 models employed are in general agreement on changes in surface and bottom temperature, whereas bottom current does not seem strongly impacted under any climate scenario.

The climate projections for the MPAs suggest significant changes in ocean conditions that are critical for marine species' survival and distribution in all MPAs assessed. For instance, temperature trends across all MPAs show an upward trend, with the most significant increases occurring under the SSP5-8.5 scenario. By the end of the century, temperature is projected to increase by a *minimum* of 1.5°C at the surface in the Gully and 1.9°C at the bottom in the Musquash Estuary. Notwithstanding large local changes, the degree of warming is not necessarily a proxy for the degree of impact on species (or predators and prey) that may be sensitive to temperature changes, for example. As future work, potential shifts in species distributions should be considered when evaluating existing MPAs (and neighbouring areas) that function as protected areas with static boundaries and are susceptible to change.

Salinity patterns also show some distinct changes, although they are less pronounced than temperature trends. SSP5-8.5 projects the largest changes in salinity, particularly in the latter half of the century, while SSP1-2.6 shows minimal changes. In half of the MPAs, salinity in bottom waters is projected to become less saline (Basin Head, Banc-des-Américains, and Musquash Estuary), while the other half is more exposed to Gulf Stream incursions at depth, and is projected to become more saline (Gully, Laurentian Channel, and St. Anns Bank).

MLD appears to become shallower, at least under the SSP5-8.5 scenario. This trend is consistent with surface warming, which reduces the ocean's ability to mix vertically. As MLD is an important proxy of vertical heat and nutrient distributions, it has an impact on processes like phytoplankton production and the uptake of atmospheric carbon. Continued monitoring and proactive strategies will be necessary to protect marine ecosystems from the adverse effects of climate change. As AI mapping provides a more precise, high-resolution picture of future ocean conditions, it offers critical insights for conservation and management.

5. Acknowledgements

This work is funded by the Marine Conservation Targets initiative under the project *Past and future oceanographic conditions for MPAs and OECMS in Canada's three oceans*. DFO colleagues Drs. Christine Stortini and Ryan Stanley internally reviewed the report and provided insightful inputs.

6. References

Andres, H.J., Soontiens, N., Penney, J. and Cyr, F. (2024). Seasonal variations of the cold intermediate layer on the Newfoundland and Labrador Shelf. *Progress in Oceanography*, 229, p.103379.

Boyce, D.G., Tittensor, D.P., Garilao, C., Henson, S., Kaschner, K., Kesner-Reyes, K., Pigot, A., Reyes Jr, R.B., Reygondeau, G., Schleit, K.E. and Shackell, N.L. (2022). A climate risk index for marine life. *Nature Climate Change*, *12*, 854-862.

Brickman, D. and Shackell, N.L., 2024. Phenology metrics for ocean waters with application to future climate change in the Northwest Atlantic Ocean. Elem Sci Anth, 12, 1-20, doi:10.1525/elementa.2024.00001.

Castillo-Trujillo, A.C., Kwon, Y.O., Fratantoni, P., Chen, K., Seo, H., Alexander, M.A. and Saba, V.S. (2023). An evaluation of eight global ocean reanalyses for the Northeast US continental shelf. *Progress in Oceanography*, 219, p.103126.

Czich, A.N., Stanley, R.R.E., Avery, T.S., Den Heyer, C.E. and Shackell, N.L., 2023. Recent and projected climate change–induced expansion of Atlantic halibut in the Northwest Atlantic. Facets, 8, 1-14, doi: 10.1139/facets-2021-0202.

Danielson, R. E., M. Zhang, J. Chassé, and W. Perrie (2025) A seasonal to decadal calibration of 1990-2100 eastern Canadian freshwater discharge simulations by observations, data models, and neural networks, arXiv:2506.05261 [stat.AP] (to appear in 2026, *Atmos.-Ocean*, 64, 1-16, doi:10.1080/07055900.2025.2521502).

DFO (2011) Biophysical Overview of the Laurentian Channel Area of Interest (AOI). DFO Can. Sci. Advis. Sec. Sci. Advis. Rep. 2010/076.

DFO (2022) 2021 Review of baseline information, monitoring indicators, and trends in the Gully marine protected area. DFO Can. Sci. Advis. Sec. Sci. Advis. Rep. 2022/017, (accessed May 2025 at https://science-ouverte.canada.ca/handle/123456789/279).

DFO (2025) Musquash Estuary Marine Protected Area (MPA) annual report 2023. Annual report. Musquash Estuary Marine Protected Area. 1-9 (assessed June 2025 at https://waves-vagues.dfo-mpo.gc.ca/library-bibliotheque/4127569x.pdf).

Drenkard, E.J., Stock, C., Ross, A.C., Dixon, K.W., Adcroft, A., Alexander, M., Balaji, V., Bograd, S.J., Butenschön, M., Cheng, W. and Curchitser, E. (2021) Next-generation regional ocean projections for living marine resource management in a changing climate. *ICES Journal of Marine Science*, 78, 1969-1987.

Eyring, V. and Bony, S. and Meehl, G. A. and Senior, C. A. and Stevens, B. and Stouffer, R. J. and Taylor, K. E. (2016). Overview of the Coupled Model Intercomparison Project Phase 6 (CMIP6)

experimental design and organization. *Geosci. Model Dev*., 9, 1937-1958, doi:10.5194/gmd-9-1937-2016.

Faille, G., Côté, G., Blais, M., Gagné, R., Chamberland, J.-M., Galbraith, P.S., Dazé Querry, N., Lehoux, C., Ricard, D. and Starr, M. (2023). DFO Monitoring Indicators for the Banc-des-Américains Marine Protected Area: Review, Choice of Measures and State of Knowledge. DFO Can. Sci. Advis. Sec. Res. Doc. 2023/067. xi + 147 p.

Ford, J., and Serdynska, A., Eds. (2013). Ecological Overview of St Anns Bank. Can. Tech. Rep. Fish. Aquat. Sci. 3023: xiv + 252 p.

Greenan, B. J. W., James, T. S., Loder, J. W., Pepin, P., Azetsu-Scott, K., Ianson, D., Hamme, R. C., Gilbert, D., Tremblay, J.-É., Wang, X. L., Perrie, W. (2019). Changes in oceans surrounding Canada, Chapter 7 of Canada's Changing Climate Report, E. Bush and D. S. Lemmen, Eds., Government of Canada, Ottawa, Ontario, p. 343–423, (accessed April 2024 at https://changingclimate.ca/CCCR2019).

IPCC (2021). Summary for Policymakers. In: Climate Change 2021: The Physical Science Basis. Contribution of Working Group I to the Sixth Assessment Report of the Intergovernmental Panel on Climate Change [Masson-Delmotte, V., P. Zhai, A. Pirani, S. L. Connors, C. Péan, S. Berger, N. Caud, Y. Chen, L. Goldfarb, M. I. Gomis, M. Huang, K. Leitzell, E. Lonnoy, J.B.R. Matthews, T. K. Maycock, T. Waterfield, O. Yelekçi, R. Yu & B. Zhou (eds.)]. Cambridge University Press.

Innes, M., E. Saba, K. Fischer, D. Gandhi, M. C. Rudilosso, N. M. Joy, T. Karmali, A. Pal, and V. B. Shah, (2018). Fashionable modelling with Flux, arXiv:1811.01457 [cs.PL].

Joseph, V., Thériault, M.-H., Novaczek, I., Coffin, M., Cairns, D., Nadeau, A., Boudreau, M., Plourde, M.-A., Quijon, P.A. and Tummon Flynn, P. (2021). Review of monitoring activities in Basin Head Marine Protected Area in the context of their effectiveness in evaluating attainment of conservation objectives. DFO Can. Sci. Advis. Sec. Res. Doc. 2021/044. xi + 89 p.

Keen, L.H., Stortini, C.H., Boyce, D.G. and Stanley, R.R., (2024). Assessing climate change vulnerability in Canadian marine conservation networks: implications for conservation planning and resilience. *Facets*, 9, 1-15, doi:10.1139/facets-2023-0124.

Lawlor, J.A., Comte, L., Grenouillet, G., Lenoir, J., Baecher, J.A., Bandara, R.M.W.J., Bertrand, R., Chen, I.C., Diamond, S.E., Lancaster, L.T. and Moore, N., 2024. Mechanisms, detection and impacts of species redistributions under climate change. *Nature Reviews Earth & Environment*, *5*, 351-368, doi: 10.1038/s43017-024-00527-z.

Lellouche, J.-M., E. Greiner, R. Bourdallé-Badie, G. Garric, A. Melet, M. Drévillon, C. Bricaud, M. Hamon, O. Le Galloudec, C. Regnier, T. Candela, C.-E. Testut, F. Gasparin, G. Ruggiero, M.

Benkiran, Y. Drillet, and P.-Y. Le Traon (2021). The Copernicus global 1/12 oceanic and sea ice GLORYS12 reanalysis. *Front. Earth Sci.,* 9, 1–27, doi:10.3389/feart.2021.698876.

Lewis, S.A., Stortini, C.H., Boyce, D.G. and Stanley, R.R., 2023. Climate change, species thermal emergence, and conservation design: a case study in the Canadian Northwest Atlantic. *Facets*, *8*, 1-16, doi: 10.1139/facets-2022-0191.

Loder, J. W., Baaren, A., & Yashayaev, I. (2015). Climate comparisons and change projections for the northwest Atlantic from Six CMIP5 models. *Atmosphere-Ocean*, *53*, 529–555. https://doi.org/10.1080/07055900.2015.1087836.

Maraun, D., 2016. Bias correcting climate change simulations-a critical review. *Current Climate Change Reports*, *2*, 211-220, https://doi.org/10.1007/s40641-016-0050-x.

Meehl, G. A., Covey, C., Taylor, K. E., Delworth, T., Stouffer, R. J., Latif, M., McAvaney, B., and Mitchell, J. F. B. (2007). THE WCRP CMIP3 Multimodel Dataset: A New Era in Climate Change Research, *Bull. Amer. Meteorol. Soc*., 88, 1383–1394.

McKee, E.,Wang, Z., and DeTracey, B. (2023). Evaluation of Bottom Temperature From GLORYS12 and EN4 for North American Continental Shelf Waters: From the North Atlantic, to the Arctic, to the North Pacific Oceans. Can. Tech. Rep. Hydrogr. Ocean. Sci. 355: vii + 34 p.

Mercator Océan International. (2022). *Global Ocean Physics Reanalysis*, Dataset. https://doi.org/10.48670/moi-00021.

Pinsky, M.L., Worm, B., Fogarty, M.J., Sarmiento, J.L. and Levin, S.A., 2013. Marine taxa track local climate velocities. *Science*, *341*, 1239-1242, doi:10.1126/science.1239352.Schmidt, G.A., Bader, D., Donner, L.J., Elsaesser, G.S., Golaz, J.C., Hannay, C., Molod, A., Neale, R.B. and Saha, S. (2017). Practice and philosophy of climate model tuning across six US modeling centers. *Geoscientific Model Development*, 10, 3207-3223.

Taylor, K. E., Stouffer, R. J., and Meehl G. A. (2012). An Overview of CMIP5 and the Experiment Design, *Bull. Amer. Meteorol. Soc*., 93, 485–498.

Wang, S., F. J. Murillo, and E. Kenchington (2024). Climate-change refugia for the bubblegum coral Paragorgia arborea in the northwest Atlantic, *Front. Mar. Sci.,* 9, 1-23, doi:10.3389/fmars.2022.863693.

Wang, Z., Greenan, B.J.W. (2013). Ocean circulation in the Northwest Atlantic: an evaluation of the GLORYS reanalysis. In: Canadian Technical Report of Hydrography and Ocean Sciences. Vol. 294, –vi + 31pp.

Wang, Z., Brickman, D., Greenan, B., Christian, J., DeTracey, B., and Gilbert, D. (2024). Assessment of Ocean Temperature Trends for the Scotian Shelf and Gulf of Maine Using 22 CMIP6 Earth System Models, *Atmos.-Ocean*, 62:1, 24-34, DOI: 10.1080/07055900.2023.2264832.

7. Appendix

This project provides multiple gridded products of CMIP6 model ensembles and GLORYS12 reanalysis data, along with adjusted CMIP6 projections. Data averages are also provided (i.e., over MPAs and for multiple timescales from monthly to 20-years in length). An example is the NetCDF file

maritime_mpa_20_year_climatology.nc

This file contains the 20-year climatology average and standard deviation for each of the variables mentioned in this report (also listed below) for each grid cell in the MPA regions.

Variables:	**dimensions**
Gully	11 x 9 x 4 x 48 x 12
Laurentian	34 x 28 x 4 x 48 x 12
StAnnsBank	17 x 10 x 4 x 48 x 12
BasinHead	3 x 2 x 4 x 48 x 12
Americains	7 x 6 x 4 x 48 x 12
Musquash	4 x 3 x 4 x 48 x 12
Gully_lat	9 x 1
Gully_lon	11 x 1
Laurentian_lat	28 x 1
Laurentian_lon	34 x 1
StAnnsBank_lat	10 x 1
StAnnsBank_lon	17 x 1
BasinHead_lat	2 x 1
BasinHead_lon	3 x 1
Americains_lat	6 x 1
Americains_lon	7 x 1
Musquash_lat	3 x 1
Musquash_lon	4 x 1
Time	48 x 1

Dimensions = lon, lat, SSP, time, parameter

Where: SSP(1) = SSP1-2.6; SSP(2) = SSP2-4.5; SSP(3) = SSP3-7.0; SSP(4) = SSP5-8.5
Time = 12 months for each 20-year period

parameter(1) = SST;	parameter(2) = SST std;
parameter(3) = BT;	parameter(4) = BT std;
parameter(5) = SSS;	parameter(6) = SSS std;
parameter(7) = BS;	parameter(8) = BS std;
parameter(9) = MLD;	parameter(10) = MLD std;
parameter(11) = bottom current speed;	parameter(12) = bottom current speed std